

南華大學科技學院永續綠色科技碩士學位學程

碩士論文

Master Program of Green Technology for Sustainability

College of Science and Technology

Nanhua University

Master Thesis

應用有限元素法於辛樂克颱風導致之深層崩塌邊坡穩定分析

Using Finite Element Method on the Stability Analysis of Rainfall-

Induced Deep-seated Landslide triggered by Typhoon Sinlaku

許柏瑞

Akash Chakraborty

指導教授：洪耀明 博士

Advisor: Yao-Ming Hong, Ph.D.

中華民國 110 年 5 月

May 2021

南華大學
永續綠色科技碩士學位學程
碩士學位論文

應用有限元素法於辛樂克颱風導致之深層崩塌邊坡穩定分析
Using Finite Element Method on the Stability Analysis of Rainfall-Induced
Deep-seated Landslide triggered by Typhoon Sinlaku

研究生：Akash Chakraborty

經考試合格特此證明

口試委員：

張光宗

凌耀明

尹孝元

指導教授：凌耀明

系主任(所長)：李敏

口試日期：中華民國 110 年 5 月 28 日

ACKNOWLEDGEMENT

Numerous thanks to the many who have provided support, encouragement, and advice throughout the writing of this thesis and my time at Nanhua University.

First and foremost, I would like to convey my sincere gratitude to my thesis advisor Professor Hong Yao-Ming of the Department of Green Technology for Sustainability, Nanhua University. His constant patience, guidance, suggestions, and motivation throughout this research have been vital to the learning experience of this research field. It has been a great privilege and honor to work and study under his guidance.

I am indebted to my master thesis defense committee members for their insightful comments and valuable suggestions. I would like to acknowledge our department professors, academic and lab assistants for aiding me during this research period, may that be learning new courses, documentation work or laboratory experiments. I would also like to thank my friends and classmates for consistently being a source of inspiration and support. You are all amazing and have been a highlight of my time at Nanhua University. I will treasure the memories.

Ultimately, I must offer my heartfelt gratitude to my parents for their unwavering support and everlasting encouragement throughout my academic and general life. This accomplishment would not have been possible without them.

Author

Akash Chakraborty

Master Program of Green Technology for Sustainability, Nanhua University

摘要

地滑帶來危險的地質災害，除導致生命損失外，也會破壞基礎設施，導致供水、通訊和醫療設施等重要設施無法使用。邊坡穩定性分析可預測自然邊坡的強度及可靠度的關鍵技術。本研究結合有限元素法與剪應強度降低技術，發展多物理場模型來分析地滑地之穩定，並模擬惠蓀林場的地滑事件，其中達西定律，被用來尋找流體在土壤之孔隙壓力及流率，並以莫爾庫倫定律分析地理彈性及塑性。此研究中，以有限元軟件 COMSOL 多重物理量模式，對降雨誘發的滑坡進行了耦合水力及大地之邊坡穩定分析，並以降雨、孔隙水壓力和地下水位擾動引起的土壤運動條件，比較崩塌前後高程與模擬成果，了解其準確性。結果表明，崩塌地穩定取決於地質、地形、邊坡幾何形狀、土壤類型和邊坡材料。水文和地文因子變化，會導致邊坡穩定度隨土壤強度參數的降低。本研究有助於預測臨界地下水位、壓力流線和位移，幫助大地工程師和災害專家發展早期預計系統，防止災難性滑坡的發生並減輕下坡造成的災害。

關鍵詞：降雨誘發地滑、邊坡破壞、水力大地耦合分析、地下水位

ABSTRACT

A landslide is a geological hazard that is perilous and a bringer of misfortunes. A landslide event will induce the loss of lives and infrastructure along with the non-availability of important facilities like water supplies, communication lines, and medical facilities. Stability analysis is a crucial technique, which can predict the strength and reliability of natural slopes. This study developed a Multiphysics model to analyze the stability of a deep-seated translational slide. The Finite Element Method combined with the shear strength reduction technique was used to simulate the landslide event for the Huisun forest area. Darcy's law was used to find the pore pressure and the flow rate of fluid in the soil. The geo-elastoplastic analysis was governed by the Mohr-Coulomb failure criterion. A coupled hydro-geotechnical slope stability analysis was carried out for a rainfall-induced deep-seated planar landslide slope by utilizing a finite element software COMSOL Multiphysics. The soil movement due to rainfall, pore water pressure, and groundwater level fluctuations was investigated. The landslide zone of pre/post landslide were compared with simulation outcome for accuracy estimation. Results indicated that the slope stability of the slide depended on the geology, topography, slope geometry, soil type, and slope materials. The slope stability reduces with the decrease of soil strength parameters due to hydrological and geotechnical factors. This study contributes to the prediction of critical groundwater level, pressure flow-lines, and displacements which can be used as key monitoring indices for the development of early warning systems by soil engineers and disaster experts to prevent catastrophic landslide occurrences and mitigate the disasters caused in the downslope.

Keywords: rainfall-induced landslide, slope failure, hydro-geotechnical coupled analysis, groundwater level

TABLE OF CONTENTS

ACKNOWLEDGEMENT	I
摘要	II
ABSTRACT	III
TABLE OF CONTENTS.....	IV
LIST OF FIGURES	VII
LIST OF TABLES	IX
LIST OF ABBREVIATIONS.....	X
Chapter 1 Preface	1
1.1 Introduction	1
1.2 Objective.....	5
Chapter 2 Literature Review	8
2.1 Factors triggering landslides	8
2.2 Types of landslide movement & failures	12
2.3 List of landslides	14
2.4 Traditional analysis methods.....	16
2.5 Modern analysis methods	17
2.6 Summary of past research.....	19
Chapter 3 Theory	23
3.1 Infinite Slope Stability Theory	23
3.1.1 Darcy's law	23
3.1.2 Laplace's Equation of Continuity	24
3.1.3 Mohr-Coulomb Failure Criterion.....	25
3.1.4 Elastic properties and constants	28
3.1.5 Groundwater level fluctuation	30
3.2 Multiphysics Simulation Concepts	31
3.2.1 Finite Element Method (FEM)	31

3.2.2 Pore pressure	33
3.2.3 Shear Strength Reduction Method (SSRM)	35
3.2.4 Factor of Safety (FOS).....	36
Chapter 4 Methodology	38
4.1 Study Area.....	38
4.1.1 Location	38
4.1.2 Topography and climate	39
4.1.3 Geology and structure	40
4.1.4 Landslide & typhoon history	42
4.2 Materials and Software	42
4.2.1 Elevation data of study area.....	42
4.2.2 Rainfall data	44
4.2.3 Sieve Analysis (Grain size distribution).....	45
4.2.4 COMSOL Multiphysics software	50
4.2.5 QGIS software	51
4.3 Parameters and assumptions for Simulation.....	51
4.4 Initial & Boundary conditions	53
4.5 Procedure flow chart	55
4.6 Gravity loading	56
Chapter 5 Results & Discussion	57
5.1 Preprocessing and Data Conversion	57
5.2 Numerical Model Creation	60
5.3 Meshing of the Model.....	62
5.4 Slope Stability Analysis.....	66
5.4.1 Subsurface Flow Analysis	66
5.4.2 Geo-mechanical Analysis	68
5.4.3 Coupled Hydro-Geo-mechanical Simulation	71
5.5 Significance of this research	80
5.6 Applicability of the proposed method	81

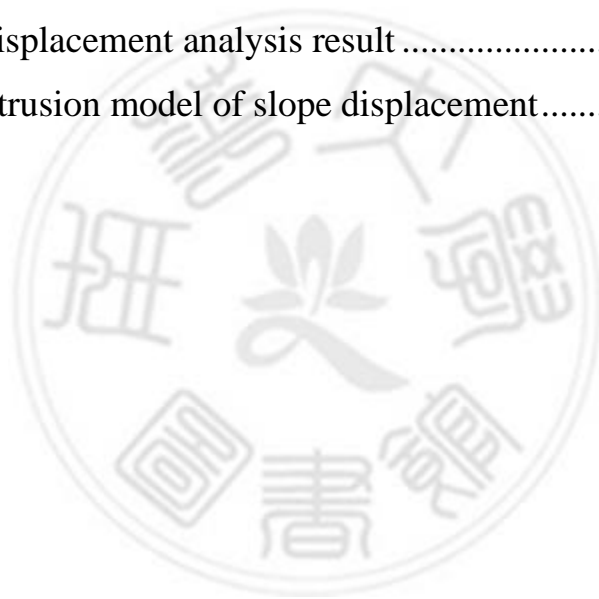
5.7 Shortcomings and future scope.....82
Chapter 6 Conclusion.....83
References.....85
Appendix90
Appendix 1: Sieve analysis data90



LIST OF FIGURES

Figure 1-1: Cross-section of a landslide occurring slope	2
Figure 1-2: 3-D view of a slope failure.....	3
Figure 2- 1: Landslide types	13
Figure 3-1: Diagram portraying Darcy’s law	23
Figure 3-2: Diagrams depicting shear and normal stresses	25
Figure 3-3: Mohr-Coulomb failure Diagram	26
Figure 3-4: Three-dimensional stress loading	28
Figure 3-5: Pore-water pressure mechanism	34
Figure 4-1: Study area photos (Taken in March 2021).....	39
Figure 4-2: Study area location.....	40
Figure 4-3: Geological profile	41
Figure 4-4: Rainfall Depth & Cum. Rainfall vs Date	44
Figure 4-5: Site investigation points	46
Figure 4-6: Particle size distribution curve.....	48
Figure 4-7: Course of action flow chart.....	55
Figure 5-1: 2007 DTM data	58
Figure 5-2: 2009 DTM data	58
Figure 5-3: 2013 & 2018 DTM data	59

Figure 5-4: Elevation difference graph between different years	60
Figure 5-5: Model geometry	61
Figure 5-6: Two-dimensional linear triangular elements diagram	63
Figure 5- 7: Nodal displacement for triangular element.....	63
Figure 5-8: Model meshing.....	65
Figure 5-9: Pressure head analysis result.....	73
Figure 5-10: Pressure analysis result	74
Figure 5-11: Von-mises stress analysis result.....	75
Figure 5- 12: Effective strain analysis result	77
Figure 5- 13: Total displacement analysis result	78
Figure 5- 14: 2-D Extrusion model of slope displacement.....	78



LIST OF TABLES

Table 1: Climatic factors activating landslide	8
Table 2: Hydrological factors activating landslide	9
Table 3: Geotechnical factors activating landslide	11
Table 4: Landslide Inventory	15
Table 5: Past research synopsis.....	19
Table 6: Failure envelope description.....	27
Table 7: Site GPS points and elevations	47
Table 8: Sieve collector pan retained percentage	49
Table 9: USDA particle size chart	49
Table 10: Grain size distribution analysis results	50
Table 11: Geotechnical analysis framework.....	53
Table 12: Simulation predictions	79

LIST OF ABBREVIATIONS

Abbreviation	Meaning
FEM	Finite element method
FEA	Finite element analysis
FOS	Factor of safety
GWL	Groundwater level
CGWL	Critical groundwater level
SSR	Shear Strength Reduction
SRF	Strength reduction factor
GLF	Groundwater level fluctuation
SSA	Slope stability analysis
LEM	Limit equilibrium method
DOF	Degree of freedom
USGS	United States Geological Survey
USDA	US Department of Agriculture
I-D	Intensity- Duration
IDF	Intensity-duration-frequency

Chapter 1 Preface

1.1 Introduction

Landslide is a slope failure event caused due to natural disasters, physical events, and sometimes man-made. The most destructive landslides are rainfall-induced, earthquake-induced, and volcanic-induced landslides. The other types include storm-induced, snowmelt-induced, and human-caused landslides. Landslides have been a widespread natural calamity in Taiwan, China, Japan, Hong Kong, Italy, India, etc. due to their extreme terrain conditions and diverse climatic actions like heavy rainfall enhanced by typhoons and cyclones (Gattinoni, 2008; Hong & Wan, 2011; Zhang et al, 2011; Zhou et al, 2014; Chen et al, 2017). These landslides, if unnoticed, can cause excessive loss of life and infrastructure thus, making it a major concern for the world population (Pradhan et al, 2019). Landslides account for considerable loss of life and damage to human settlements, communication networks, agricultural farmlands, forests, and other essential facilities. They mostly occur in seismically active regions with rough mountainous terrain accompanied by high orographic precipitations and frequent earthquakes (Okeke & Wang, 2016). Slope failures are mostly associated with destabilizing events such as substantial rainfall, tectonic activities, and erosion. Rainfall-induced landslides have increased with time due to various rainfall activities all across the world (Cai & Ugai, 2004; Monsour et al, 2011). The effects of pore pressure due to rainfall infiltration and the mechanical behavior of both saturated and unsaturated slopes have now become an important research interest (Leshchinsky et al, 2015). Deep-seated landslides are mostly caused due to increasing positive pore-water pressure on the slip plane induced by an escalating GWL (Van Asch et al, 1999). A rainfall-induced landslide depends on two types of rainfall i.e., torrential rainfall and prolonged rainfall. Torrential rainfall is powerful, rapid, and finishes fast while the prolonged rainfall

may not be always strong but takes place for longer durations. Both affect the slope surface differently and ultimately leads to destabilization. The destabilization types are mostly Coulomb loading or liquefaction (Ghiassian & Ghareh, 2008). After going through many papers, it has been seen that the researchers have concluded that rainfall-induced landslide is a complex activity as a lot of aspects change when rainfall takes place. Different terrains have different strengths and weaknesses which further depend on many other hydro-geotechnical properties (Wu et al, 2014). Therefore, it is important to know how the various factors will affect the natural slope stability. Fig. 1-1 and Fig. 1-2 portrays a slope where landslide took place in 2-dimensional and 3-dimensional view.

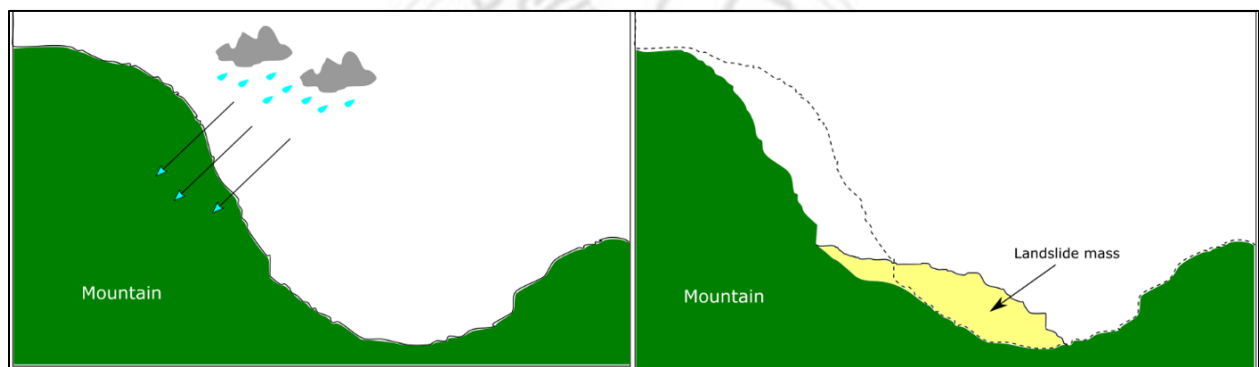


Figure 1-1: Cross-section of a landslide occurring slope

Stability of slope refers to the potential of a slope to counter slope failing forces and its withstanding capacity. This SSA is a topic of study and research in geotechnical engineering, soil mechanics, and engineering geology (Matsui & San, 1992). SSAs include static or dynamic, logical or experimental methods to evaluate the stability of natural slopes, embankments, excavated slopes, earth, and rock-fill dams. These studies are involved in the perception of slope failure movements and interpreting their triggering factors. The analyses eventually assist in preventing the origination of such movement, slowing it down, or restricting it

through diminution countermeasures. Slope stability and seepage analysis of the landslide slope is very important to determine the structural stability. (Pham et al, 2013). The stability of the landslide slope depends on the topography, geomaterials, soil or rock component properties, and the driving forces to which it is subjected. The consequent typhoon incursions, tectonic movements, and climate change impact has induced great amounts of landslides and floods posing great threats to human life and infrastructure. Many major typhoons like typhoon Morakot, Masta, Kalmaegi, Jangmi, Haitang, etc which have occurred in Taiwan has caused many landslides and flood damages. In our case, the rainfall-induced deep-seated translational landslide was caused by the typhoon Sinlaku during the year 2008.

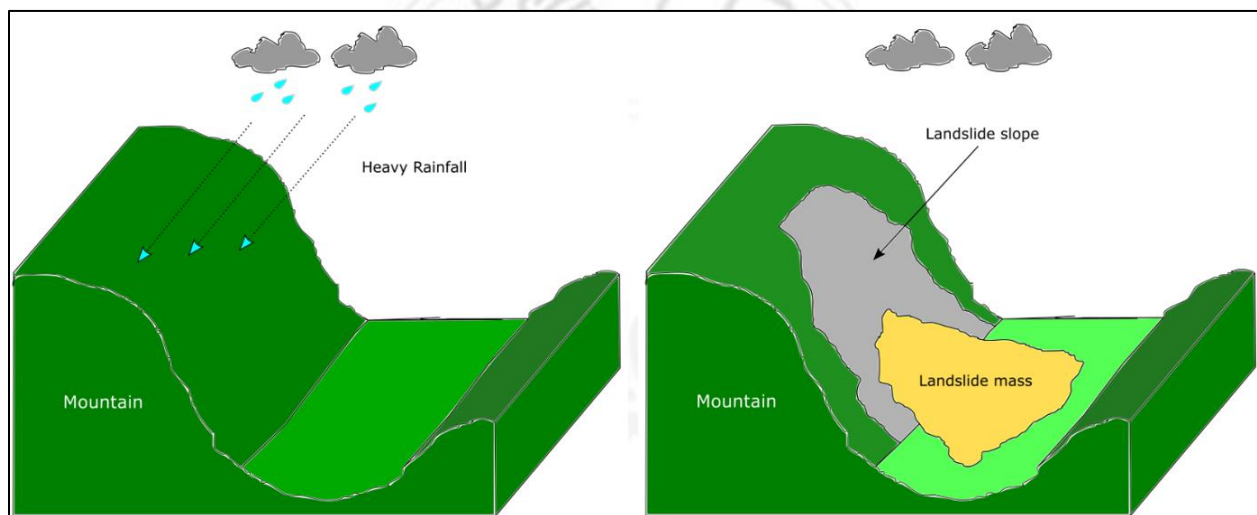


Figure 1-2: 3-D view of a slope failure

Along the passage of time, many researchers have investigated and conducted analyses to find which factors have major impacts on landslide occurrence and natural slope failures. Some recent studies concluded that uneven topography, geo-hydrological properties, boundary constraints like permeability, and the primary state of the slope are the vital triggering elements in slope failures. The methods for SSA have evolved from the traditional limit equilibrium method (LEM) to the

modern widespread numerical analysis methods, such as the finite element method (FEM), finite difference method (FDM), boundary element method (BEM), discrete/distinct element method (DEM), material point method (MPM), and numerical manifold method (NMM) (Ishii et al, 2011; Leshchinsky et al, 2015; Jeong et al, 2017; Wang et al, 2020). Activation of rainstorm-induced landslides are often been examined using physical approaches and statistical approaches. The physical approaches rely strongly on investigational results and laboratory experimental details, like the soil strength factors and geometry. As for the statistical approach, it mostly depends only on the landslide directory and precipitation data. The water pore pressure variations in the sliding material are responsible for the generation of partial liquefaction (Chang et al, 2017). The usage of finite element methods in seepage and SSAs have gained admiration lately, due to its aptitude to operate complex issues. Many researchers have been using the FEM for these types of analyses for a long time due to its fine accuracy and a good grasp of the physical facts involved.

Climate changes have also become a profound effect to cause instabilities in slope. Global warming taking place around the world is affecting the regional climate and changing it. Abrupt storms and cyclones bring heavy rainfall which induces landslides without any warnings. The projected climate changes the location, abundance, activity, and frequency of landslides in different areas. Geo-hydrological hazards like landslides, floods, and droughts are the results of these climatic variations. Landslides are a kind of mass-wasting process in slopes that accompanies serious threats to the population, but on the other hand, are important for the evolution of landscapes. Heat waves, glacial retreats, and permafrost degradation affect slope stability in high mountains (Gariano & Guzzetti, 2016). It is high time to research the slope stability and factors inducing the landslide on a

slope. However, despite the wealth of research done so far, not much has been reported about the exactness of the critical groundwater lines and landslide displacement analyses. Most of the aforementioned studies have assumed the CGWL by guess and no pre-or post-analysis has been done on the landslide-prone areas. In places where a lot of landslide disasters take place, designing an early warning system is crucial to save lives and protect infrastructure. The design or modeling of landslide slope requires many ruminations and calibrations before starting detailed SSAs. Warning schemes for landslide movements are dependent on the hydrological and geotechnical parameters. Thus, to understand these natural phenomena and their behaviors it is important to do a long-term deep observation. In this research, the slope stability of a natural slope area was investigated by FEA combined with the reduced shear strength technique.

1.2 Objective

Heavy storms, typhoons, and cyclones are common in the summer and rainy seasons of Southeast Asia and many other countries around the Pacific Ocean. They cause many landslides and slope failures during these natural wind disasters. The annular number of landslides occurring in the mountainous regions of these countries is always high posing a serious threat to the people and severe damage to the country's infrastructure and economy over the years. Numerous deterministic, probabilistic, and statistical analyses have been done for slope stability analyses over the years. For simulating a landslide model, both hydrological and geo-mechanical analyses must be done for acceptable results. The physical process of infiltration of rainfall and seepage of water through the soil has been studied by hydrogeologists, soil scientists, and geotechnical researchers in this field of landslides. The Darcy law is used in these kinds of hydraulic analyses of landslide occurrence as it is simple and accurate. The Mohr-Coulomb considers the soil model homogenous and better

for faster analysis of landslide mass. The infiltration during rainfall events leads to the rise of GWL, increase in pore water pressure, and reduction of matric suction of unsaturated soils. These mechanisms further lead to a decrease in the shear strength of soil, thus losing its stability and causing landslides and slope failures. The failure can be either shallow or deep-seated depending on the hydrological and geotechnical features of the specified area (Cai & Ugai, 2004). Many crucial facilities are built on the natural slopes like buildings & settlements, highways, railways, bridges, dams, communication lines, and water supply pipelines. The occurrence of a potentially damaging phenomenon, such as landslide in these slopes makes aforesaid facilities vulnerable and causes a lot of damage to the country and people living in it. The more the displacement range, the more is the damage range. Therefore, mitigation measures are important and can be based on the preliminary estimates of slope stability analysis (Monsour et al, 2011).

In this paper, a Multiphysics model slope stability analysis was conducted and compared with the real case to check the GWL range and corresponding soil movement due to seepage erosion and high groundwater level. The proposed research conducted a numerical analysis where the pore pressure in slopes was computed by the FEA of subsurface flow. The coupled hydro-geotechnical analyses were carried out by utilizing a finite element software COMSOL Multiphysics. Based on the results of tests conducted in this paper, the landslide occurrence area in the downstream section of the slope was demonstrated. The numerical model was calibrated with the topographical, geotechnical, and precipitation data based on the finite element theory to capture the destabilization and associated movement of the slope. The numerical model employed Darcy's law equation for subsurface flow analysis which includes the transient seepage analysis and rainfall consequences whereas the Mohr-coulomb failure criterion was implemented for elastoplastic solid

mechanics analysis which is comprised of the shear stresses and strains affecting the slope. The SSR technique was also engaged for the FOS calculation. The resulting model provided insight into the complex behavior of a progressively falling slope. It demonstrated that the use of numerical methods like FEM which allows coupling of both hydrological and geotechnical analyses present a great means of evaluating the slope stability of slopes. This research also presents a comprehensive experimental solution that evaluates the critical groundwater line range, the critical C and Phi values, the displacement range, and the structure of failure of a slope prone to landslides. The correlations between stress, strain, subsurface flow lines, pore pressure, seepage pressures, displacements, and FOS were checked and recorded. Finally, the results obtained at the end of the simulations were recorded and compared with real case observational data for verification and accuracy impact.

Chapter 2 Literature Review

2.1 Factors triggering landslides

The landslide occurrence is governed by a series of factors. Some of them are easy to acquire while others are very hard to get hold of due to their complex nature and inconsistency. Some factors are dependent on other components and change drastically. The factors causing failure are different for shallow and deep-seated landslides. The triggering phenomena are related to many interrelated factors like groundwater, lithology, infiltration, land cover, morphology, and drainage area. The climate, water features, and soil characteristics are interconnected to each other and are collectively responsible for the failure of slopes. After examining several research papers, some of the critical factors related to rainfall-induced landslides are divided into climatic, hydrological, and geotechnical factors and are enumerated in Tables 1,2 & 3 respectively.

Table 1: Climatic factors activating landslide

Factors	Author	Explanation
Rainfall intensity	Cai & Ugai, 2004; Monsour et al, 2011; Wei et al, 2019	Greater the rainfall intensity, greater the probability of occurrence of landslide on a slope surface.
Total precipitation	Baum & Godt, 2010; Hong, 2017	The rainfall amount directly affects the GWL fluctuation. The saturation of the soil body depends on it.
Air temperature	Gariano & Guzzetti, 2016	Temperature plays a major role in the landslides of tall ice mountains. Air

		temperature favors snowmelt, increasing rapid snow melting and increase runoff in the slopes.
Wind speed & duration	Gariano & Guzzetti, 2016	Wind removes soil moisture and lateral supports of slope and enhances cracking.
Meteorological invariability	Gariano & Guzzetti, 2016; Froude & Petley, 2018	This causes widening of fissures and rock jointed slopes, reduction of cohesion, and angle of friction.

The hydrological factors have an important role in landslide triggering.

Table 2: Hydrological factors activating landslide

Factors	Author	Explanation
Groundwater level variation	Hong & Wan, 2011; Wei et al, 2020	The GWL fluctuation plays a critical role in many landslides. Landslides transpire when the GWL reaches the critical GWL.
Water infiltration	Zhang et al, 2011; Leshchinsky et al, 2015; Chang et al, 2017	The infiltration is directly proportional to the rise of GWL. Excessive infiltration creates a risk of landslide.
Permeability	Gattinoni, 2009	High values of permeability increase the groundwater discharge leading to destabilization of the slope.

Pore-water pressure	Collins & Snidarcic, 2004	Higher pore pressures generate seepage forces inside the soil body, rendering the slope surface weaker.
Seepage forces & erosion	Jeong et al, 2017	It is directly proportional to the positive pore pressure and inversely proportional to the matric suction, mostly in unsaturated soils.
Hydraulic gradient	Gattinoni, 2009; Okeke & Wang, 2016	It is a driving force that governs the direction of GWL discharge, hence having a hand in landslide initiation.
Seepage velocity	Okeke and Wang, 2016	The seepage velocity increases the seepage erosion inside the soil body.
Surface runoff	Baum & Godt, 2010	If the topsoil is exposed due to less or no vegetation, the runoff impact after rainfall will make the slope susceptible to erosion and rill formations.
Soil drainage	Gattinoni, 2009	Excessive soil drainage can reduce the strength of the slope. On the other hand, less drainage leads to high GWL which can also cause a landslide.
Evapotranspiration	Gariano & Guzzetti, 2016	It affects the infiltration rate of the soil and the time for GWL rise.

If there is a lack of proper drainage systems, the fluid flow, and the pore pressure will endanger the slope stability. The permeability diverges with different types of soils and rocks, hence necessary for groundwater flow analysis and slope stability. Water is one of the main causes of landslide, thus the hazard assessment has to consider the hydrological constituents i.e., groundwater setting, and its effect on the slope stability (Gattinoni, 2009).

Table 3: Geotechnical factors activating landslide

Factors	Author	Explanantion
Slope geometry	Leshchinsky et al, 2015	Different slopes have different stabilizations depending on their geometries.
Geomaterial properties	Zhang et al, 2011; Leshchinsky et al, 2015	Different properties like the soil type, size, and composition bring about different types and timings of slope destabilization.
Soil strength parameters	Van Asch et al, 1999; Ishi et al, 2012, Zhou et al, 2014	The soil strength is governed by the cohesion value and angle of friction. Their values directly affect the soil stress and strain formations.
Matric suction	Cascini et al, 2013; Okeke and Wang, 2016	Matric suction changes the effective stresses in soil which have a direct impact on soil stability. Slope aspect and soil thickness produce regional differences in soil suction.

Reactivation	Chen et al, 2017; Pradhan et al, 2019	The reactivations are caused in the old landslide area where the soil has already lost its strength and are dangerous.
Bedrock conditions and lithology	Gattinoni, 2009; Leshchinsky et al, 2015	If there is a loose soil cover over a rigid bedrock, a landslide will most likely occur in these types of slopes.
Geomorphology	Wu et al, 2014; Chen et al, 2017	Changes in landforms due to weathering and erosion affect the slope strength.
Land cover	Baum & Godt, 2010	The presence or absence of vegetation on natural slopes plays a vital role in stability.

A high soil erosion rate can decrease the response time of the slope area. A small variation of any one factor can establish a big result on the whole soil structure involved. Some researchers even considered the rainfall kinetic energy as a factor for stability analyses. High intensity rainfall has higher rainfall kinetic energy and can accelerate the soil erosion process (Chang et al, 2017). Typhoons have a huge impact factor to trigger landslides as it generates more rainfall intensity and speeds up the failure process. (Wu et al, 2014; Hong, 2017).

2.2 Types of landslide movement & failures

Landslide movement is divided into 4 types i.e., fall, slide, spread and flow. A detailed chart for landslide types according to the USGS is given in Figure 2-1.

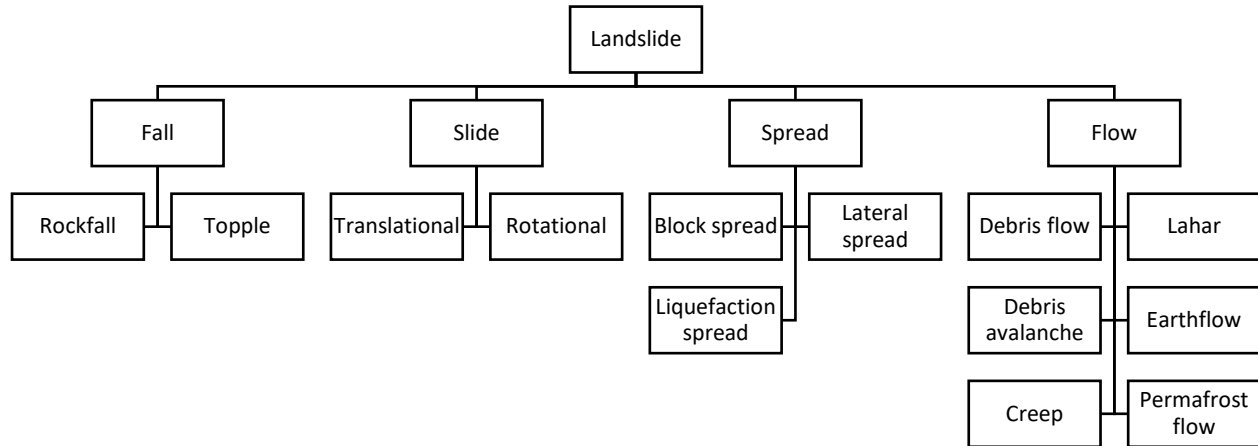


Figure 2- 1: Landslide types

The fall generally occurs when the shear resistance of the slope becomes almost zero and it falls. Slopes comprised mostly of rock experience rock avalanches and rockfalls. The topple or rotational slide is when a soil or rock mass rotates around an axis that lies below the soil mass. The translational slide is a downslope movement where intense shear strain has taken place but is relatively thinner than the other types. Spread is caused on cohesive soils when the underlying soil is softer than the upper soil and extends accompanied by subsidence. Flows are rapid movements but have thicker composition than a slide. Debris flows are an example of flow-type movements. The movement is similar to a viscous fluid (Monsour et al, 2011).

Some researchers emphasized that the failure in natural soil slopes and rock jointed slopes are different. In soil slopes, a little displacement may trigger landslide but that is not the case in rock slopes (Wang et al, 2020). A displacement or rock movement in a rock jointed slope doesn't imply that it will become unstable. Soil is plastic or elastic while rocks are rigid. A rigid body has more stability; hence both soil and rock slopes need to predict the displacements around the potential slip surface which will give more accuracy. Finite element modeling is good for soil

slopes since they are continuum-based numerical methods but for rocks, discontinuous model analysis is needed.

In many places, the previous landslide events cause a threat of reactivation of the landslide in the same area. The reactivation happens almost several times in the old landslide zone. Every reactivation creates more fear and different types of damage. Hence this repetitive nature of landslides is a major concern too. The hydrological changes accelerate/decelerates the reactivation of landslide zones (Pradhan et al, 2017). For example, sometimes rainfall-induced landslides occur in volcanic environments where the soil is unconsolidated and weak due to previous volcanic events (Crosta & Frattini, 2008). The series of landslides that occur in these volcanic slopes make the geomaterial composition weaker every time. The surfaces of weakness like faults, cracks, joints, and bedding planes control the failure. Seepage forces exceed intergranular stresses or cohesion forces, thus causing detachment and movement of soil particles (Ghiassian & Ghareh, 2008). Nevertheless, the accuracy of the landslide displacement and GWL analysis is filled with uncertainties due to its complex wavering nature of slope and soil parameters. It is crucial to do the pre-slope stability analysis and mitigate these failures and reactivations.

2.3 List of landslides

Landslides have been a relentless natural disaster activity among many countries with different timings of slope failure. They are mostly triggered due to physical phenomena like rainfall and earthquakes. A list has been made depicting some of the landslides acquired from the literature.

Table 4: Landslide Inventory

Trigger & depth type	Researcher	Landslide name/Study area	Landslide type	Country	Cause
Rainfall-induced; Deep-seated	Mantovani et al, 2000	Tessina landslide	Rotational and translational slide	Italy	Groundwater level change
	Gattinoni, 2008	Cavallerizzo landslide	Complex debris slide with earth flow	Italy	Groundwater rise; prolonged rainfalls
	Hong and Wan, 2011	Lu-Shan landslide	Translational slide	Taiwan	Haitang and Masta typhoons
	Wu et al, 2014	Xiaolin landslide	Translational slide and debris flow	Taiwan	Typhoon Morakot
	Zhou et al, 2014	Ercengyan landslide	Rotational and translational slide	China	Water table fluctuations; High rainfall
	Hong, 2017	Wu-She Reservoir	Translational slide	Taiwan	Sinlaku & Jangmi typhoon
	Wei et al, 2019	Duxiantou landslide	Translational rockslide	China	Torrential precipitation
	Wei et al, 2019	Huayuan landslide	Translational slide	China	Heavy rainfall; Groundwater level fluctuation
Rainfall-induced; Shallow	Leshchinsky et al, 2015	Yumokjeong landslide	Translational slide	South Korea	Excessive rainfall
	Jeong et al, 2017	Umyeonsan landslides	Translational slides with debris flow	South Korea	Heavy rainfall

	Chang et al, 2017	Shihmen, Xiayun and Jiaxian area	Translational slides with debris flows	Taiwan	Typhoon Kalmaegi
	Pradhan et al, 2019	Kotropi landslide	Debris flow and translational slide	India	Heavy rainfall; Reactivation of landslide
Earthquake-induced; Deep-seated	Wu et al, 2014	Tsaoling landslide	Translational rockslide	Taiwan	Chi-Chi 1999 earthquake
	Wu et al, 2014	Chiufenershan landslide	Translational slide	Taiwan	Chi-Chi 1999 earthquake
	Chen et al, 2017	Aso-ohashi landslide	Translational rock slide and debris flows	Japan	Kumamoto 2016 earthquake
	Chen et al, 2017	Futagawa and Hinagu fault areas	Translational rock slide	Japan	Kumamoto 2016 earthquake

2.4 Traditional analysis methods

All the research for soil stability analyses started with the use of traditional quantitative and statistical methods. The most popular ones are the limit equilibrium methods and method of slices. These traditional methods have been modified with time by new researchers for the SSA. Classical slope stability approaches like sliding block method, circular method of slices, log-spiral, etc. neglects many factors like the slope kinematics, principal stress redistributions, dissipation of suction stresses, and pore pressure formations (Leshchinsky et al, 2015). Negligence of these many factors will consequently decrease the accuracy and will become incompetent for real case analysis and practical uses.

The LEM is one of the most widely used traditional methods to calculate the stability of slopes and stress analysis of geotechnical structures. It utilizes the

method of slices which is very popular in practical landslide engineering. This procedure can merge complex slope geometries, variable soil properties, different boundary load condition influences, and pore water conditions. The method of slices had been used for a long time in this field. It comprises the ordinary slices method and the Bishop's Modified method. Other quantitative methods include the friction circle method and the Fellenius method. Fellenius's method consists of 3 steps i.e, determining the failure slip surface, estimation of axial force, and calculating the FOS of slope (Matsui & San, 1992). The most widely used statistical methods were the Bayesian inference method and the frequentist approach. These 2 methods are mostly used in mathematical calculations of the I-D thresholds. Every method has its dependent factors and governing equations.

The problem of all equilibrium methods is that they all are based on the same assumption that the soil mass can be divide into slices which in turn demands more assumptions. The limitation of LEM methods is that it can only calculate the resultant force for a single point and not for the whole force distribution which affects the different deflections at various parts of the slope, shear forces, and bending moments acting on the slope surface. Hydro-mechanical problems tend to have many complexities. FEM has a benefit over non-linear analyses like slope stability because it considers various parameters and can support the coupling of different physical studies.

2.5 Modern analysis methods

Traditional methods have the problem of explaining non-linear problems. It causes trouble when the model has complex geometry or excessive variation of materials. Hence, to counter these problems, the methods have been revised over the years and evolved, uncovering many new modern methods. The traditional methods have got outdated and modern methods have taken the place. The relation between

rainfall and GWL affecting the slope stability is generally complicated since many external factors affect which is not possible to include in a statistical approach like evapotranspiration, the intensity of rainfall, morphology of slope, and the thickness of saturated zone. To date, GWL fluctuation prediction is mostly predicted by 3 approaches: physical model, phenomenological/statistical model approach, and data mining/machine learning approach. (Wei et al, 2019).

Numerical analysis is done for a variety of many complex problems since they are fast and easy to use. It is a robust method for composite problem solutions. FEM is a numerical method that has been used constantly for its fine performance and accurate results. The landslide is a phenomenon that is related to different factors and fields. Many hydrological and geo-mechanical components collectively affect the slope towards failure. Therefore, it is important to conduct a coupled geo-hydrological slope analysis. In the traditional methods, it is mostly impossible or very difficult to combine different fields and find results. The FEM and the other modern numerical methods fill this gap, augmenting its precision and reliability. The other modern methods for slope stability include the discrete element method (DEM), finite difference method, boundary element method (BEM), linear reservoir method (LSM), material point method (MPM), numerical manifold method (NMM), impulse response method (IRM) and general particle dynamics (GPD). Many researchers around the world use different approaches to increase their research model accuracy. The DEM is good for estimating the slope stability of rock slopes (Wang et al, 2020). It is an iterative determination process based on a statistical criterion to establish the FOS.

The modern statistical methods include regression model analysis and I-D threshold curve modeling. In I-D modeling, a separation line is drawn visually or by separation techniques to serve as a probabilistic transition zone between

precipitation events that induce landslides and events that do not involve such hazards. They are fast since not many physical concepts are required but have reduced accuracy. Nowadays numerical analysis methods are combined with data mining techniques or artificial intelligence for superlative stability analyses. The data mining techniques encompass the artificial neural network (ANN) method and support vector machines (SVM). In the artificial intelligence field, ANNs have high popularity for application in various fields, whether it is in the computer science field like adaptive control, image analysis, voice recognition, etc., or in the geotechnical field for black-box slope stability analysis (Hong, 2017). Accurate predictions of landslide triggering events can be done and they can learn fast based on small samples. It has been found that when using these data mining techniques, it is governed by FEA techniques. Hence FEM remains one of the superior modern methods for slope stability analyses to date.

2.6 Summary of past research

The literature studied and examined prior to the research is catalogued below in Table 5.

Table 5: Past research synopsis

Investigator	Discussion	Criteria
Matsui & San, 1992	The SSR technique was developed and used for slope stability analysis	The SSR method was compared with results of Bishop's method and verified with Fellenius' method

Cai & Ugai, 2004	The hydraulic characteristics of soil were computed and analyzed	The FEA of transient water flow was used for the analysis
Collins & Znidarcic, 2004	Prediction of depth and relative time of failure of slopes due to infiltration was done	The infinite slope analysis and one-dimensional flow modeling was used for failure identification
Ghiassian & Ghareh, 2008	Numerical seepage analyses were conducted for 2 different cases of sandy slope – with and without horizontal drains and the effects were checked	The infinite slope model was used for the translational slope movement analysis for 2 types of slope destabilization – Coulomb loading & static liquefaction
Baum & Godt, 2010	The hydro-geotechnical features of the early warning systems from the past till now were studied and summarized	Several landslide warning systems of USA along with their history, technical problems, and accuracy were investigated
Hong & Wan, 2011	A model to predict the GLFs along a hillslope in response to hourly precipitation rate was established	The linear reservoir method along with governing Darcy's law equation was used for the forecasting analysis
Mansour et al, 2011	The researchers tried to relate the scope of damage to the cumulative displacement of the landslide mass	50 cases of slow-moving slides were studied and their damage extent due to their vulnerability

		was checked using some elementary statistics
Ishii et al, 2012	The shear strength of the sliding surface was analyzed and a ratio called stability index was formulated for SSA	An elasto-viscoplastic constitutive model was implemented using FEM for investigating the slope deformations and safety factors
Cascini et al, 2014	The relationship between rainfall type, soil suction, and initiation of slope instabilities involving pyroclastic soils was established	All the rainfall data and geological data were acquired from the Campania region landslide database and rainfall thresholds were calculated
Leshchinsky et al, 2015	The continuous movement of a shallow landslide was examined with the help of measured soil data and precipitation calibration	A numerical model was employed with Bishop's effective stress approach for the transient seepage analyses and deformation study analyses
Gariano & Guzzetti, 2016	The effects of climatic variations on the failure of slopes were studied	Many published works were reviewed to probe the past, current, and expected impact of climate change on landslides
Jeong et al, 2017	The geomorphological features and spatial distribution of	The seepage analyses were done using SWCCs and all the results were compared with integrated

	precipitation- induced landslides were studied	laboratory analysis and numerical analyses
Pham et al, 2018	This study deduced that the SWCC model and permeability values play a critical role in SSAs	The SWCCs were calculated using the pressure-plate extractor test and Tempe model
Pradhan et al, 2019	This study conducted simulations and assessment of the stability grades of the slope and mitigation measures were discussed	The finite element modeling was used for the stability simulations and SRFs were derived for verification of stability analyses
Wang et al, 2020	The slope stability of jointed rock slopes was analyzed and the FOS and SRFs were calculated and verified	DEM was implemented for stability analysis and verified with the results of FDMs
Wei et al, 2020	This study examined and compared the accuracy of GWL variation prediction performance between 2 models	The physical model was run by a FE seepage code-named Slide and the phenomenological model used was PSO-SVM

The abbreviations of NIED denotes National Research Institute for Earth and Science and Disaster Resilience of Japan, PSO-SVM denotes signify Particle Swarm Optimization – Support Vector Machine and SWCC indicate Soil-water characteristic curve.

Chapter 3 Theory

3.1 Infinite Slope Stability Theory

3.1.1 Darcy's law

Darcy's law is a governing equation that describes the movement of fluids in a porous medium. Darcy's law is valid for both unsaturated and saturated soils (Cai & Ugai, 2004). The equation for Darcy's Law is derived from the observations that the flow rate through a porous medium (such as an aquifer) is proportional to the cross-sectional area perpendicular to flow and is also proportional to the head loss per unit length in the direction of flow. The diagram Fig. 3-1 below illustrates the Darcy's law.

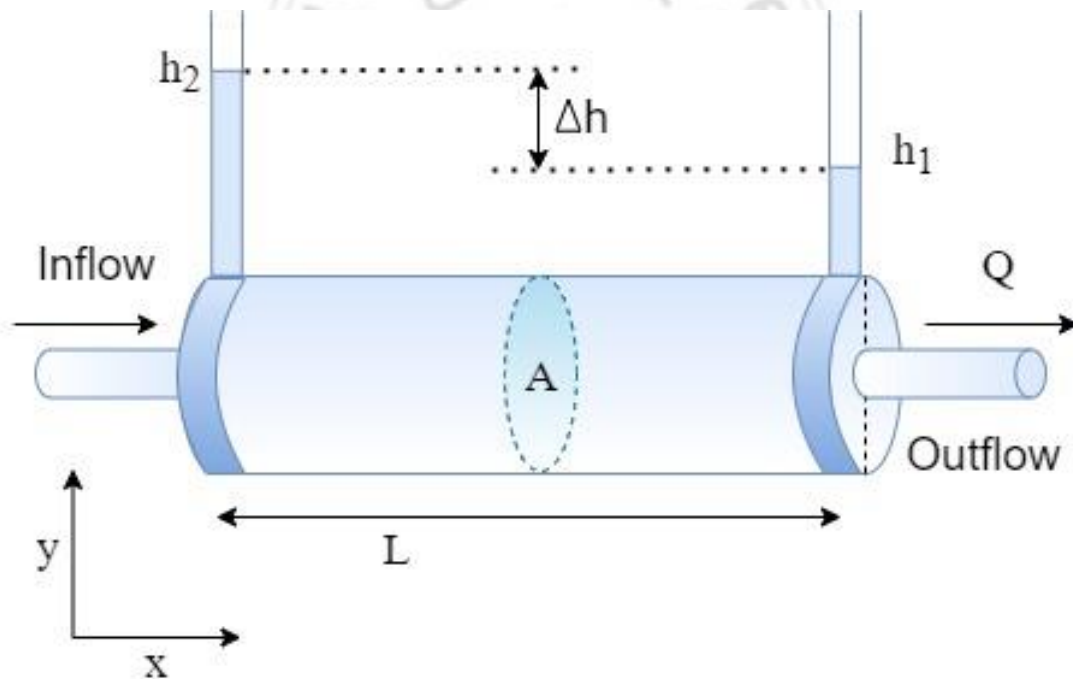


Figure 3-1: Diagram portraying Darcy's law

Darcy's law equation is-

$$Q = KAh_i \quad (1.1)$$

The hydraulic gradient h_L is shown as –

$$h_i = \frac{h_2 - h_1}{L} = \frac{\Delta h}{L} \quad (1.2)$$

Where, Q is the flow rate of liquid through the porous medium, A is the cross-sectional area perpendicular to flow, L is the horizontal length of flow and K is hydraulic conductivity. The hydraulic conductivity, K , is a constant for a given porous medium. A very porous medium with little resistance to flow will have a high value for K , while a tightly packed medium with high resistance to flow will have a low value for K .

3.1.2 Laplace's Equation of Continuity

The hydrological analysis conducted in this research combined the Darcy's law with the Laplace's equation of continuity to govern the steady flow condition for a given point in a soil mass. It describes the motion of water in soil (Hong and Wan, 2011). This equation arises from a consideration of mass conservation in an unsaturated-saturated medium coexistent with an equation of motion. The hydrological continuity equation is formulated as:

$$\frac{dS}{dt} = I_r - O_r \quad (1.3)$$

Where I_r is the inflow rate of water due to various factors like infiltration, surface runoff, etc. and O_r is the groundwater outflow rate. S is the groundwater storage in respect to time t . The transport of fluids through a porous medium, for example, seepage water and soil, is often resisted by the pore fluids present in the medium reducing the momentum of transport. Darcy's law is a method that can be used to model this situation. Darcy's law combined with a continuity equation can

be used for a hydrological case analysis, which in our case is the GLF and seepage water flow through the porous landslide model. It is a complete mathematical model which can be used to describe the fluid movements through the gaps and spaces present inside the porous mediums. The application of this continuity model is suitable for cases related to landslide slopes, aquifers, riverbanks, soil embankments, etc. where the pore water effects are a major factor.

3.1.3 Mohr-Coulomb Failure Criterion

The Mohr-Coulomb failure criterion is the representation of the linear envelope that is obtained from a plot of the shear stress of a material versus the applied normal stress. The Mohr-Coulomb failure criterion is a set of linear equations in principal stress space, where the conditions will make any isotropic material fail. Figure 3-2 and 3-3 depicts the stress formation and Mohr-Coulomb formulation.

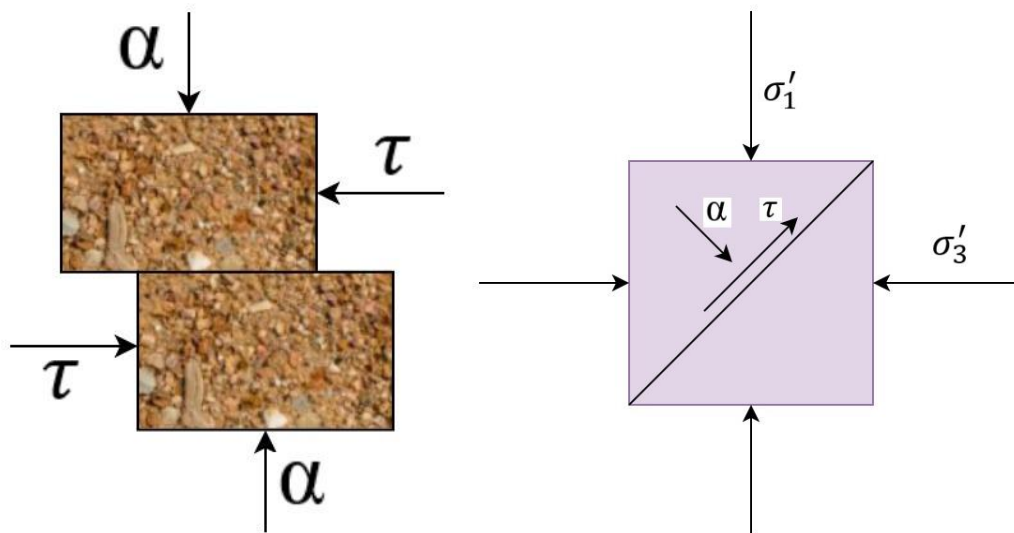


Figure 3-2: Diagrams depicting shear and normal stresses

The Mohr-Coulomb model is defined by-

$$\tau = c + \alpha \tan \Phi \quad (2.1)$$

Where, c is the cohesion of soil, Φ being the angle of internal friction, α is the normal stress and τ is the shear stress of soil. The failure criterion (Griffiths and Lane, 1999) is defined by –

$$F = \frac{\sigma'_1 + \sigma'_3}{2} \sin \phi - \frac{\sigma'_1 - \sigma'_3}{2} - c \cos \phi \quad (2.2)$$

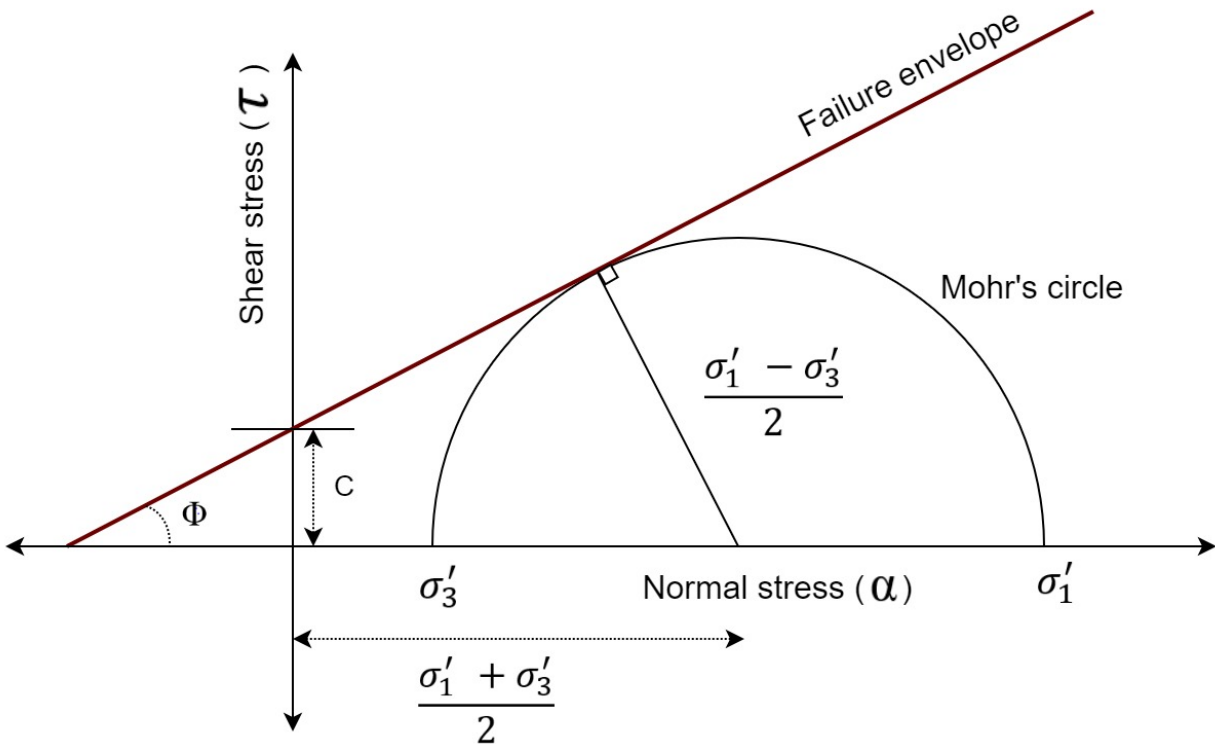


Figure 3-3: Mohr-Coulomb failure Diagram

Where, σ'_1 is the major principal effective stress, σ'_3 as the minor principal effective stress and F is the failure function. If the stresses at a particular Gauss point stay within the Mohr-Coulomb failure envelope, then that position is assumed to remain elastic. If the stresses lie over or exterior of the failure envelope, then that

position is assumed to be yielding. The value of failure criterion affects the soil stress strength parameters as shown in Table 6.

Table 6: Failure envelope description

Failure criterion function	Interpretation
$F < 0$	Stresses inside failure envelope (elastic)
$F = 0$	Stresses on failure envelope (yielding)
$F > 0$	Stresses outside failure envelope (yielding and must be redistributed)

Failure can be different for different types of simulations: bulging of the slope profile, limiting of the shear stresses on the potential failure surface, or non-convergence of solutions. Non-convergence means that the solution algorithms are no longer able to converge within the user-limited number of iterations, which implies that no stress distribution can be found and the model is experiencing failure. The slope failure and non-convergence occur simultaneously when the two solutions Mohr-Coulomb failure criterion and global equilibrium cannot be satisfied simultaneously. This non-convergence or failure causes an increase in nodal displacements within the mesh (Griffiths and Lane, 1999). In the case of models where the geological composition is mostly rocks, the generalized Hoek-Brown criteria are used for modeling. The slope failure is directly proportional to the shear strain failure criterion (Matsui & San, 1992).

3.1.4 Elastic properties and constants

The elasticity of soil is defined as the ability of the soil to recover its original shape and size after external stresses acting on it are removed. According to Hooke's law of elasticity -

$$E = \frac{\alpha_0}{\varepsilon_0} \quad (3.1)$$

Where, α_0 is the stress and ε_0 is the strain acting on the material, the four moduli were formed i.e., elasticity modulus (E), bulk modulus (k), shear modulus (G), and constrained modulus (CM) (Lambe & Whitman, 1991). The different moduli have their respective diagrams and equations. In this research, the isotropic loading was considered which has been described by Fig. 3-4.

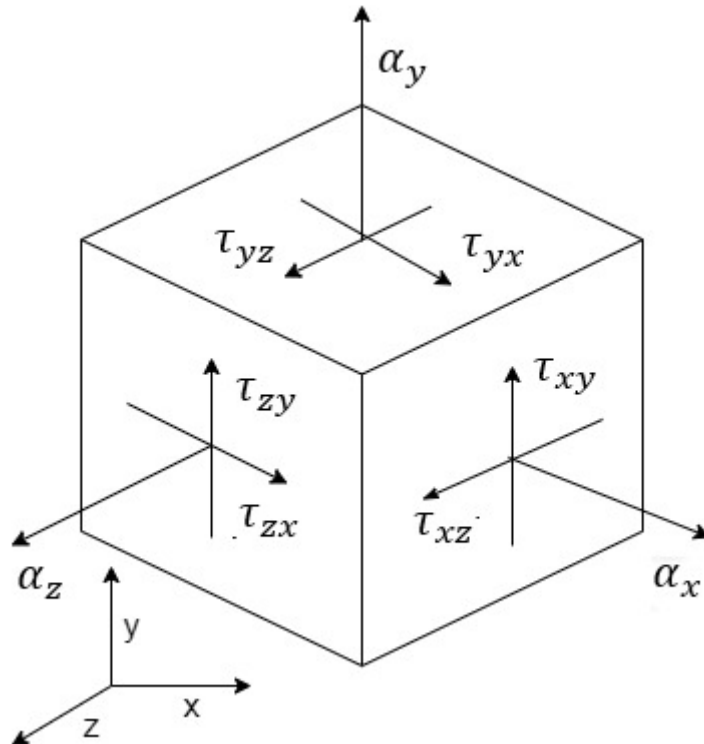


Figure 3-4: Three-dimensional stress loading

In case of constrained modulus, the equation stands as:

$$CM = \frac{\alpha_x}{\varepsilon_x} \quad (3.2)$$

The strains in a 3-D structure were calculated in accordance to Hooke's law and principle of superpositions (Lambe & Whitman, 1991) as shown as –

$$\varepsilon_x = \frac{1}{E} [\alpha_x - v(\alpha_y + \alpha_z)] \quad (3.3a)$$

$$\varepsilon_y = \frac{1}{E} [\alpha_y - v(\alpha_x + \alpha_z)] \quad (3.3b)$$

$$\varepsilon_z = \frac{1}{E} [\alpha_z - v(\alpha_x + \alpha_y)] \quad (3.3c)$$

Where, v is the Poisson's ratio of soil. The volumetric strain is –

$$\frac{\Delta V}{V} = \varepsilon_x + \varepsilon_y + \varepsilon_z \quad (3.4)$$

For an isotropic case all the stresses are equal i.e., $\alpha_x = \alpha_y = \alpha_z = \alpha_0$, then the volumetric strain becomes –

$$\frac{\Delta V}{V} = \frac{3\alpha_0}{E} (1 - 2v) \quad (3.5)$$

Therefore, the constrained modulus of x direction can be calculated by setting the other two directional strains as zero i.e., $\varepsilon_y = \varepsilon_z = 0$ –

$$\alpha_y = \alpha_z = \frac{v}{1 - v} \alpha_x \quad (3.6)$$

$$CM = \frac{1}{m_v} = \frac{E(1 - v)}{(1 + v)(1 - 2v)} \quad (3.7)$$

The equation used for calculating the elastic parameters i.e., Young's modulus and Poisson's ratio for this hydro-mechanical analysis,

$$E = \frac{(1 + \nu)(1 - 2\nu)}{m_\nu(1 - \nu)} \quad (3.8)$$

Where, m_ν is the coefficient of volume compressibility i.e, the inverse of constrained modulus. The derivations are shown above. The elastic parameters are crucial in the soil mechanics analysis since it has a profound influence over the deformations before failure but have a very little influence on the factor of safety prediction in the slope stability analysis. Hence if there is no original data, nominal data values can be put ($E = 10^5 \text{ kN/m}^2$ and $\nu = 0.3$) (Griffiths & Lane, 1999).

3.1.5 Groundwater level fluctuation

GWL rises when infiltration takes place. During rainfall, the rainwater collected on the topsoil surface tries to penetrate the soil due to gravity and the tendency of water to pass through pervious objects. After traveling some time, they finally reach the aquifer region where the groundwater is stored. This process is known as infiltration of rainwater. The total inflow of water in soil is dependent on many positive and negative factors. According to some researchers (Hong & Wan, 2011) the simple equation for this total water inflow I_f is given by –

$$I_f = I_t + A_r - S_r - R_s \quad (3.9)$$

Where, I_t is the total infiltration, A_r as the total rainfall amount, S_r is the surface runoff and R_s is the retention of water in pores of soil. Therefore, when heavy rainfall or long-duration rainfall takes place more water infiltrates, and the GWL rises faster. Finally, when the GWL reaches the CGL, the soil slope becomes unstable and a landslide will be activated. The GWLF defines as the difference

between the present time and the next time GWL. (Hong, 2017). The sudden rise of GWL due to heavy rainfall is a major factor in the occurrence of landslides (Wei et al, 2020). Typhoons have a great impact factor to trigger landslides since they bring heavy rainfall. Therefore, it is important to create a real-time prediction system to forecast the landslide occurrence (Wu et al, 2014). When a landslide occurs, there is generally no time to evacuate or protect, thus SSA must be done from before for safety. Thus, it is important to evaluate its failure timing beforehand.

An important fact was discovered after going through the references i.e., while comparing the rainfall with the GWL data there is a time lag between the time when the maximum precipitation occurs and the time when the GWL was at its peak. This happens due to 2 mechanisms. Firstly, the time taken for the whole rainwater accumulated on the topsoil to infiltrate the soil and reach the groundwater storage is mostly dependent on the hydraulic conductivity of the soil. Secondly, the groundwater drainage due to seepage or piping inside the hillslope reduces the groundwater storage thus lowering the GWL. Some studies related to SWCC model analyses deduced that the hydraulic behaviors and properties like permeability, also play a critical role in slope stability of a slope surface under unsaturated seepage circumstances and GWLFs (Pham et al, 2018).

3.2 Multiphysics Simulation Concepts

3.2.1 Finite Element Method (FEM)

FEM has been widely accepted in the research field of hydraulic and geotechnical engineering for many years. Elastoplastic analysis of geotechnical problems and sub-surface flow analysis related to hydraulic problems are nowadays mostly simulated using FEA. Slope stability represents an area of hydro-geotechnical analysis in which a nonlinear FE approach offers real benefits over existing

traditional methods. (Griffiths & Lane, 1999), (Matsui & San, 1992) The graphical capabilities of FE programs also allow a better understanding of the mechanisms of slope failure, simplifying the output from reams of paper to manageable graphs and plots of displacements. The advantages of a FE approach to slope stability analysis over traditional limit equilibrium methods can be summarized as follows:

1. Assumptions before analysis related to the shape or the failure location are inessential, unlike the traditional methods. FEA does not require a prior guess of the critical location or surface whereas in LEM, prerequisites related to some experience of the user to locate or assume the appropriate critical slip circle is needed.
2. It is a fast and rigorous modeling technique where high accuracy can be achieved even with fewer input data.
3. Since FEM does not utilize the concept of slices there is no need of assuming slice side forces which is a common assumption in LEM. FEM preserves global equilibrium until failure condition is reached. The slice method is not accurate on the occasion of real cases.
4. If real field data are available the numerical analysis combined with FE solutions can give better results on deformation, displacement, progressive failure including overall shear failure.
5. The FEM can monitor progressive failure and overall shear failure for an entire slope distribution.

The FEM analysis has always given good prediction results and is recommended by many previous researchers. (Griffiths & Lane, 1999). FEM has a lot of contributions in the domain of elastoplastic hydro-mechanical analyses. Linear problems like the prediction of settlements and deformations, calculations of flow

quantities due to steady seepage, effects due to consolidation, effects due to saturation, and many other issues can be solved by FEM.

3.2.2 Pore pressure

Pore pressure is one of the most vital hydrological factors affecting the stability of a slope. Infiltration of water spawns pore water that is held within gaps of soil or rock particles. These pore water under gravity load and external forces generate pore water pressures on the soil slope. This pore water pressure induces seepage forces to the soil particles inside the slope surface and ultimately lead to the destabilization of a slope. Researchers have been operating on landslide assessment and prediction in various terrains across the world. Most of them are based on different mechanisms and methods to calculate the pore pressure generated inside soil due to the infiltration of water. Various effects like positive pore pressure generation due to rainfall infiltration, multidirectional groundwater seepage into the soil, etc. need to be analyzed for slope stability analysis. The failure due to pore pressure is mostly seen in rainfall-induced deep-seated landslides. Rainfall-induced landslides generally occur in natural slopes where a residual soil mass lies over a bedrock (Collins & Znidarcic, 2004). A simple diagram Fig. 3-5, to illustrate the pore water pressure (PWP) formed inside the soil surface is shown below.

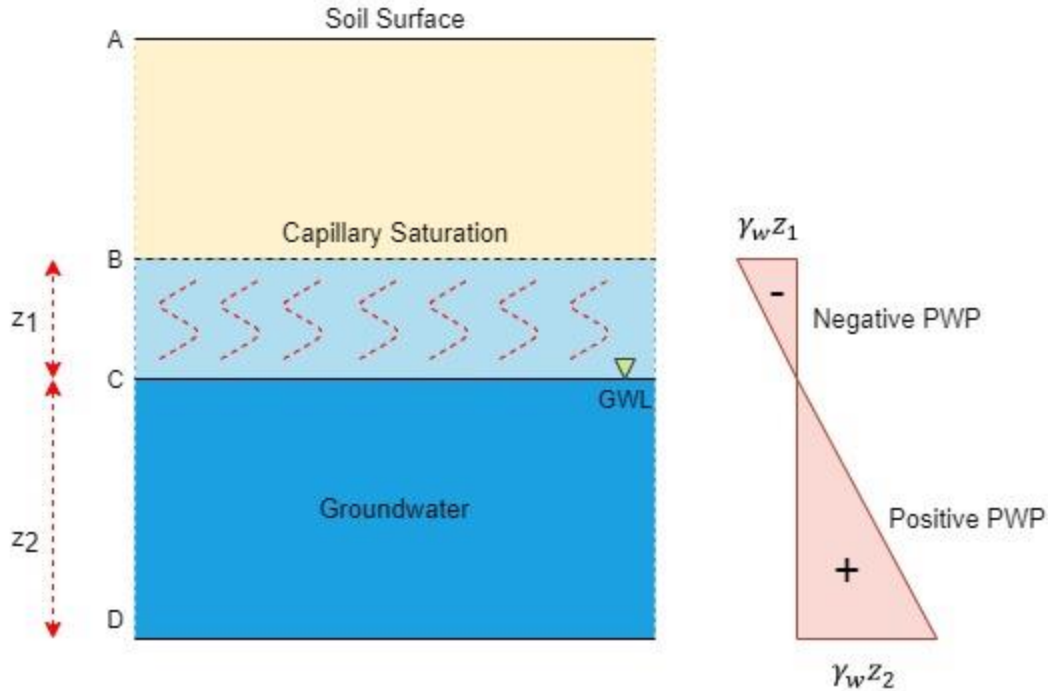


Figure 3-5: Pore-water pressure mechanism

The equation of effective stress with normal stress and PWP is given by –

$$\alpha' = \alpha + \gamma_w z_1 - \gamma_w z_2 \quad (3.10)$$

Where, γ_w is the unit weight of water. The negative pore pressure due to capillary effect gets added while the positive pore pressure is subtracted. The positive pore pressure increases with depth of the soil. In the context of FEA, the pore water pressure of a single point is determined by multiplying the unit weight of water with the vertical distance of the point beneath the free surface. The external loading of a slope structure is modeled by implementing normal stresses which are equal to the total water pressure acting on the top of upslope due to the collective rainfall amount and infiltration. As the water level increases, the applied stress increases. The applied stresses are converted to corresponding nodal loads on the FE mesh. Basically, in a FE mesh all the types of stresses like normal, effective, shear,

etc. are first converted to nodal loads and applied to the nodal points of each element on the FE mesh. It is observed in many research papers that the mechanisms for triggering deep-seated and shallow landslides were different. The deep-seated landslides of 5-20 m in depth are mostly induced due increase in pressure of pore water pressure on the slip surface since it is sensitive to rainfall. High duration and high rainfall are dangerous. For shallow landslides, the failure occurs mostly due to the reduction of cohesion of soil mass and angle of slope due to saturation of the soil. The strength of soil reduces. Matric suction is an important factor for shallow landslides but not for deep-seated landslides.

3.2.3 Shear Strength Reduction Method (SSRM)

The SSRM is used to find the safety factor value of the slope at the point of failure also called the instability point. The FOS is defined as the ratio of the available shear strength of the soil that is required to maintain an equilibrium across the surface. The FOS ratio of a slope surface demonstrates how much it can withstand the external loads, stresses, and self-weight. In the context of slope stability, the FOS would ideally be a ratio that does not lead to sliding of the materials in the slope. FOS is not a measure of the reliability of the slope, but rather gives a relative indication of the resistance to any driving forces induced within the slope stability analysis. The FOS is shown by –

$$FOS = \frac{\text{Total Shear Strength of soil}}{\text{Equilibrium Shear Stress}} \quad (3.11)$$

The equation for the reduced cohesion C' and angle of friction ϕ' is as follows:

$$C' = \frac{C}{FOS} \quad (3.12a)$$

$$\phi' = \text{atan}\left(\frac{\tan \phi_u}{FOS}\right) (p < 0) + \text{atan}\left(\frac{\tan \phi_s}{FOS}\right) (p \geq 0) \quad (3.12b)$$

Where, C is the original cohesion of soil, Φ' as the angle of internal friction, Φ_u representing the angle of internal friction in unsaturated soil, Φ_s is the angle of internal friction in saturated soil and finally, p is the pore pressure of soil. The equation considers the effect of pore water pressure on the soil strength parameters. In unsaturated soils, the pore water pressure will be less than zero ($p < 0$) while in saturated cases the pore water pressure will get included and will be more than zero ($p > 0$). The basic idea of SSRM is to divide the shear strength parameters of the soil by the SRF, reducing the shear strength of the soil mass. The method is repeated until the slope reaches a limit equilibrium state. This is the point where the SRF is considered to be the FOS of the slope. With the increasing of SRFs each time, the strength reduces and eventually converges at failure. Upon convergence, the results are determined. The friction angle of the slip zones decreases with the increasing clay content and increases with increasing gravel content.

3.2.4 Factor of Safety (FOS)

The FOS of a soil slope is defined as a number which is used to divide the original shear strength parameters (i.e., C & Φ) to bring the slope to the point of failure. The FOS is the same for the traditional limit equilibrium methods. The factored strength parameters thus become –

$$c'_f = \frac{c'}{FOS} \quad (3.13a)$$

$$\Phi'_f = \text{atan}\left(\frac{\tan \Phi'}{FOS}\right) \quad (3.13b)$$

The application of FOS is commonly used in the ‘SSR technique’ where the user can change and apply different values of FOS to the strength parameter terms.

If the FOS equals 1, the structure or part supports the exact stress it would be subjected to, and increasing or subjecting the part to any higher stress (or load) will result in the structure failing. For a FOS value of 2, the structure or part will fail at twice the working stress. If the FOS is less than 1, it means that the structure is unstable. It is found from the literature that the FOS is directly proportional to the soil strength parameters in both the LEM and FEM cases. The FEM method is very reliable and has the advantage of no requirement of prior assumption. The FOS determination is a natural process for the FE approach. The FEM is a better and powerful alternative to the traditional limit equilibrium methods (Griffiths and Lane, 1999). The FOS is insensitive to gravity loading influence in plastic Mohr-Coulomb models. It is more sensitive to the loading sequences which includes more complex laws like reproducing volumetric change in undrained or partially drained environment. The FOS of a slope can be increased by adding piles or retaining walls in the landslide zone as it increases the slope stability (Zhou et al, 2014).

Chapter 4 Methodology

4.1 Study Area

4.1.1 Location

The field data were obtained from the Huisun experimental forest, which is situated at Nantou County of Taiwan, approximately 35 km to the east of Taichung city. Fig. 4-2 represents the study area location. It is the largest experimental forest among the 4 belonging to the National Chung Hsing University. The reason for choosing this study area is because it falls under the area of Taiwan which is prone to many landslides. Some mountain sides are mostly rugged while some are covered with heavy vegetation. Some of the images that were taken during the study area visit are shown in Fig. 4-1.

In Taiwan, during the summer season, heavy torrential precipitation takes place along with many typhoons causing hazards like landslides, mudslides, and floods. The study area Huisun, located in Nantou County is subjected to all these experiences resulting in frequent GLFs thus making it a good area for research studies and analyses.



Figure 4-1: Study area photos (Taken in March 2021)

4.1.2 Topography and climate

Nantou county is a wide mountainous range with rugged terrain and steep topography. Due to the 2000-meter altitude difference in Huisun, from 450-2,420 m, the forest is longitudinally scattered between peak and valley, and so the main features of the climate can be divided into tropical, subtropical, and warm regions. Due to these variations of topographic features, various effects of climate change

and the natural disasters resulting from them can be observed and studied. The area is directly located on the convergent tectonic plate boundary between the Eurasian Plate and the Philippine Sea Plate thus making it a landslide-prone area with weak geological structures. As Taiwan lies in the north-western Pacific Ocean which is a major typhoon formation area due to its warm ocean waters, heavy torrential precipitation takes place along with many typhoons during the summer season causing hazards like landslides, mudslides, and floods (Yang & Tsai, 2019).

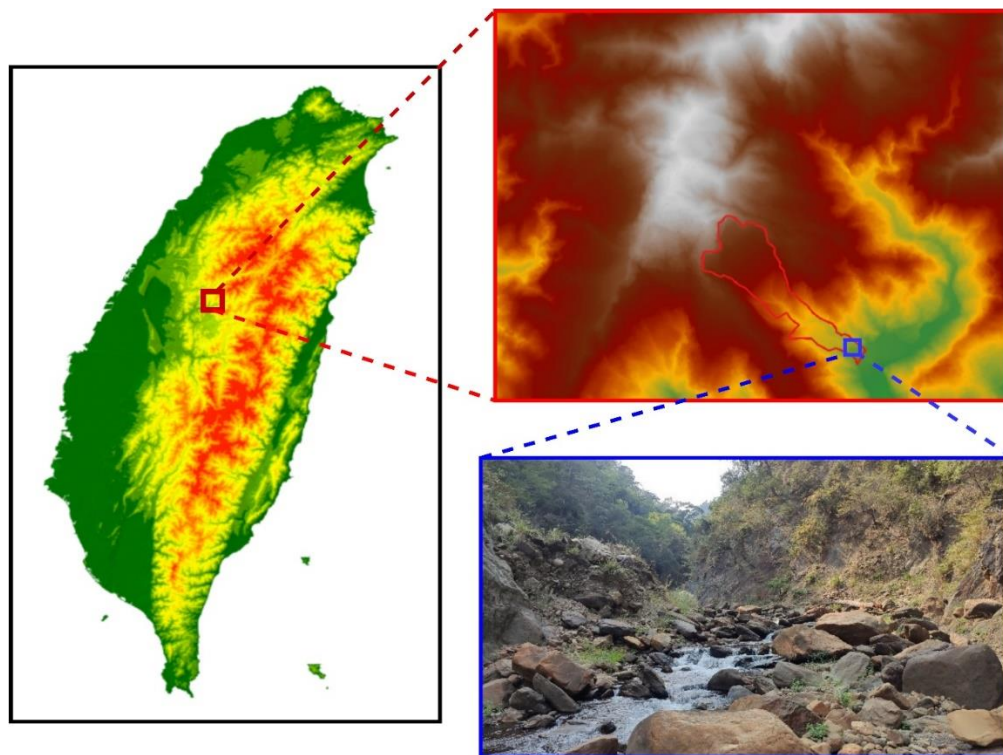


Figure 4-2: Study area location

4.1.3 Geology and structure

After going through literature related to the geology of Taiwan, it was found that the Huisun forest area falls in the Hsuehshan range of the Central Mountain range of Taiwan (Ho, 1986). The data obtained from these geological papers about

the Hsuehshan range and after doing a field visit at the study area it was found that the area consists of rocks, gravel, sand and little amount of clay and silt. The lowest layer of the mountain range was found to be comprised of high-pressured metamorphic rocks like slates, schist, and gneiss. The underlying bedrock below the soil surface is comprised of sandstone and shale. The topsoil consists of a mixture of gravel, sand, and soil. The heavy rainfalls due to typhoons cause landslides which in turn make the geological characteristics of the vicinity weaker and more permeable creating fractures and active faults with time (Chen et al, 2017). This can later give rise to the reactivation of another landslide in the same place. Therefore, it is important to analyze the slope stability and take preventive measures. Fig. 4-3 describes the geological structure of Huisun area that was assumed after going through some papers related to the geology of Taiwan (Ho, 1986; Tsou et al, 2011; Brown et al, 2012).

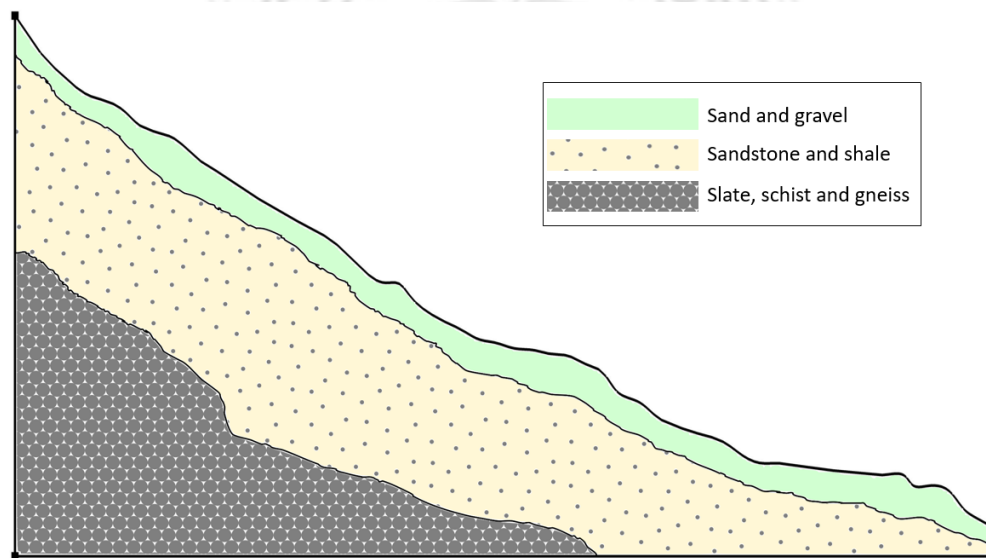


Figure 4-3: Geological profile

4.1.4 Landslide & typhoon history

The landslide event studied in this research can be classified as a translational landslide caused due to intense and prolonged rainfall. Asia is the dominating geographical area for landslide occurrences. Climate changes induce sudden rainfalls in steep slope areas causing catastrophic landslide events. Seasonality is another factor. Most landslides occur during the summer and rainy seasons. Nantou County has faced many landslides due to typhoons like Morakot (Tsou et al, 2011; Wu et al, 2014), Sinlaku, Jangmi, Haitang, etc, and earthquakes like the 1999 Chi-Chi earthquake, 2016 southern Taiwan earthquake, etc. The Asian monsoon generates tropical typhoons and cyclones from the oceans bringing heavy and long rainfall to the Southeast Asia regions (Froude & Petley, 2018). The climate trends have noticeably increased the number of catastrophic disasters such as typhoons and rainfall-induced landslides in the Nantou regions of Taiwan. (Yang & Tsai, 2019) Severe rainfall events result in substantial and unprecedented changes in the soil characteristics and thus leads to instability. The soil is composed of weathered rocks and debris making it more permeable due to the presence of many fractures, fissures, and macropores. In many cases, the landslide mass fell over a river body and blocked it, forming landslide dams. These types of landslide structures cause water supply deficiency and many other devastating problems in the affected place.

4.2 Materials and Software

4.2.1 Elevation data of study area

The analysis was executed using four types of data – the DEM of the landslide area, the geotechnical parameters which were assumed according to the soil type, the rainfall data, and the field investigation results. The image data obtained from the study area was first accessed using QGIS software. Four image data for different

years i.e., 2007, 2009, 2013, 2018 were studied. The shapefile option from QGIS was used to create a polygon to trace the landslide area out of the whole map. A line was drawn at the middle of the polygon from its top to bottom using the multiline function. After the line was created, 52 points were marked on the line with equivalent space distance for acquiring the coordinate and elevation points. The ID data of each of the points were collected and inscribed in a text file. The same process was repeated for all the four maps and all their x, y, and z points were noted down. The obtained coordinate data was used to calculate the respective distances (D) using the formula –

$$D = ((x_1 - x)^2 + (y_1 - y)^2)^{0.5} \quad (4.1)$$

The x is the previous x- coordinate value whereas the x_1 is the next x-coordinate value. The same is for the y and y_1 which are the y- coordinates. After the distance calculations were finished, the stations were calculated by adding the distances cumulatively.

$$S_1 = 0 \quad (4.2a)$$

$$S_2 = S_1 + D_2 \quad (4.2b)$$

A station is a vertical distance from the datum level to a certain height. The first station (S_1) is always kept zero to mark the datum level. S_2 is the next station which is the summation of the previous station and next distance (D_2). The first distance is kept zero to keep it as the origin. All the distance and station calculations were done in excel. After obtaining the stations, they were marked on the map for every 200 m elevations to get a better visualization and understanding of the elevation of the study map.

4.2.2 Rainfall data

Rainfall is one of the main triggers for landslide occurrence. It acts as a boundary condition for setting off instabilities in rainfall-induced slopes (Cascini et al, 2013). The rainfall that occurs during monsoon periods or typhoons facilitates the infiltration of rainwater and surface runoff. The surface runoff causes soil erosion and has a hand in shallow landslides. The other water which infiltrates increases the pore water pressure inside the soil mass. This pore water in return reduces the soil strength and causes deep-seated landslides. The pore pressure changes cause changes in the displacement rate. Deep-seated landslides sometimes undergo short periods of creep with long-term creep translations followed by sudden failure (Monsour et al, 2011). Fig. 4-4 represents the rainfall data graph collected for study.

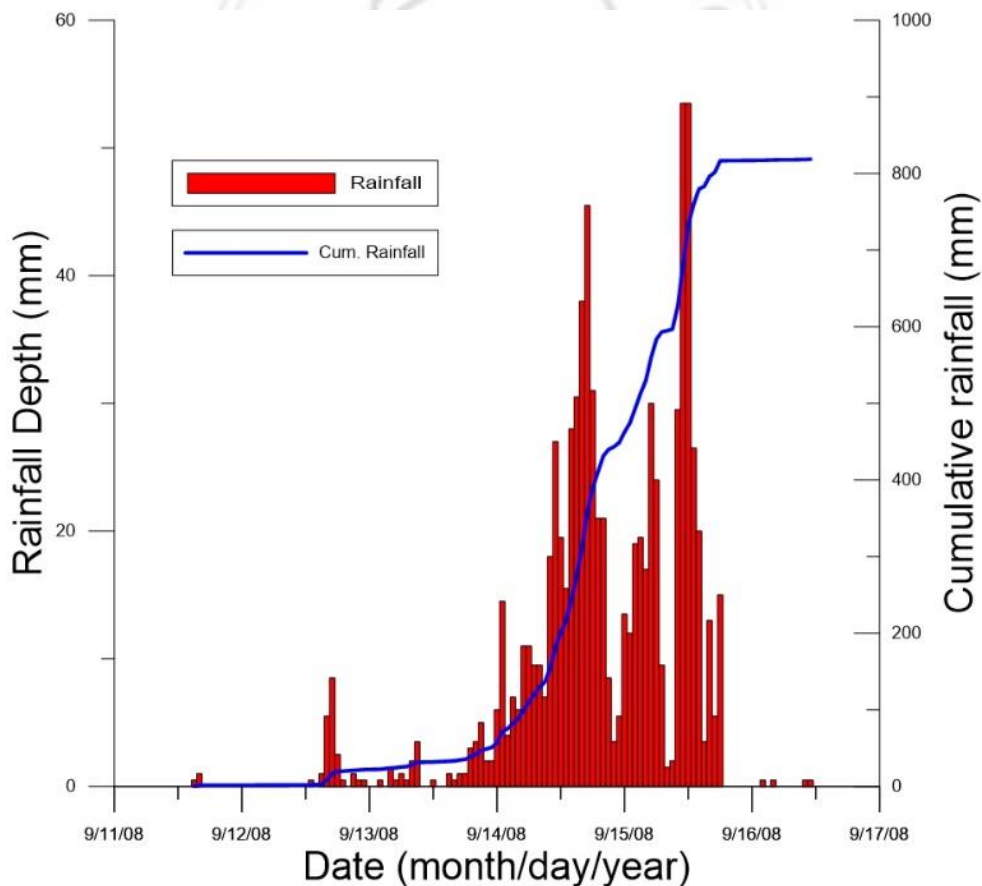


Figure 4-4: Rainfall Depth & Cum. Rainfall vs Date

The rainfall data used in this study was collected from the Central Meteorological Bureau of the Ministry of Communications of Taiwan. The observation station point was 00H81 with the address of No. 1 Shanlin Lane, Xinsheng Village (Huisun Forest Farm of Chung Hsing University), Renai Township, Nantou County, Taiwan. The distance between the rainfall observation station and the study area was approximately 3 kilometers. The data were recorded during Typhoon Sinlaku in 2008 and the groundwater level increase was analyzed using the proposed method. The slope stability is reduced with the increase of infiltration of rainfall as it decreases the shear strength of soils (Cai & Ugai, 2004). The water pressure due to rainfall was applied to the model for transient water flow finite element analysis using the rainfall data collected. Rainfall has been a vital driving force for landslide occurrence, hence, designing and installing of drainage facilities to such rainfall-induced landslide-prone slopes is a task of great importance.

4.2.3 Sieve Analysis (Grain size distribution)

Sieve analysis is a technique used to determine the particle size distribution of a sample soil. This method is performed by sifting a soil sample through a stack of wire mesh sieves, separating it into discrete size ranges. The particle size distribution of a material is important in understanding its physical and chemical properties. It affects the strength and load-bearing properties of rocks and soils. Both the field and laboratory studies were conducted to find the grain size of the landslide area. According to that, many assumptions were made in the numerical analysis. The soil sample was collected from the site, and then a sieve analysis experiment was conducted to find the mean diameter and size of the grain particles.

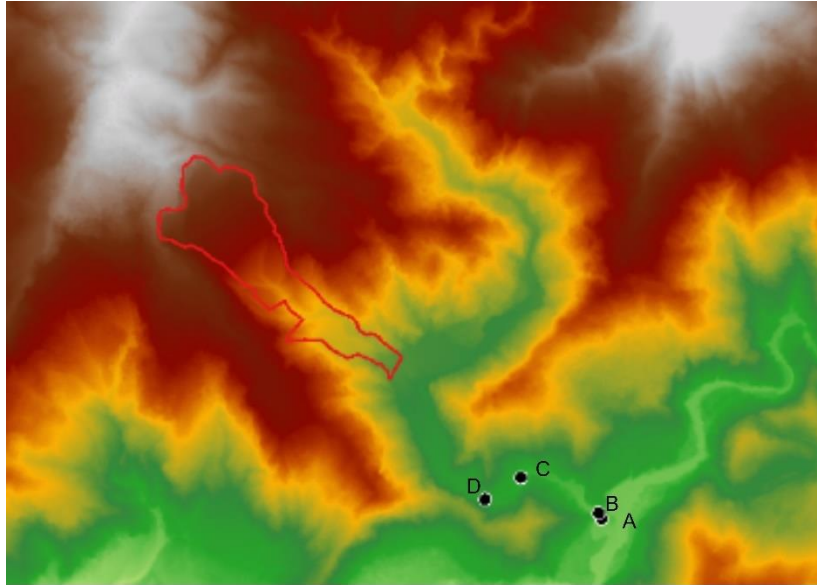


Figure 4-5: Site investigation points

The soil was collected on March 2021 from 4 points i.e., A, B, C, and D for conducting the soil particle distribution experiment as shown in Fig. 4-5. The investigation points were about 800 meters away from the toe of the landslide area. The area near the landslide slope was unstable and dangerous due to the presence of large rocks and boulders. Due to the danger and lack of safety equipment, it was decided that the soil samples should be collected at a distance from the toe of the landslide zone. We assumed that the soil was similar to the landslide slope, as regular sedimentation and weathering take place due to narrow streams present in the mountain slope. The details of the points acquired by Global Positioning System (GPS) are given in Table 7.

Table 7: Site GPS points and elevations

Sample Point	Latitude (X)	Longitude (Y)	Elevation (Z) (m)
A	252039.9	2664742.48	540.64
B	252019.79	2664780.88	541.44
C	251492.54	2665019.73	590.66
D	251248.83	2664872.79	607.51

The landslides take place due to many geo-scientific causes like sheared rock mass, old slide debris, poorly drained slope, water access, and tension crack developments which get widened with time (Pradhan et al, 2017). Hence, checking the grain size diameter is important while doing the coupled simulations. The cohesion and angle of friction values were assumed according to the mean diameter and fineness modulus obtained from the soil particle distribution analysis and used in the elastoplastic hydro-mechanical slope analysis. The sieve analysis graphs for the four points are shown below in Fig. 4-6.

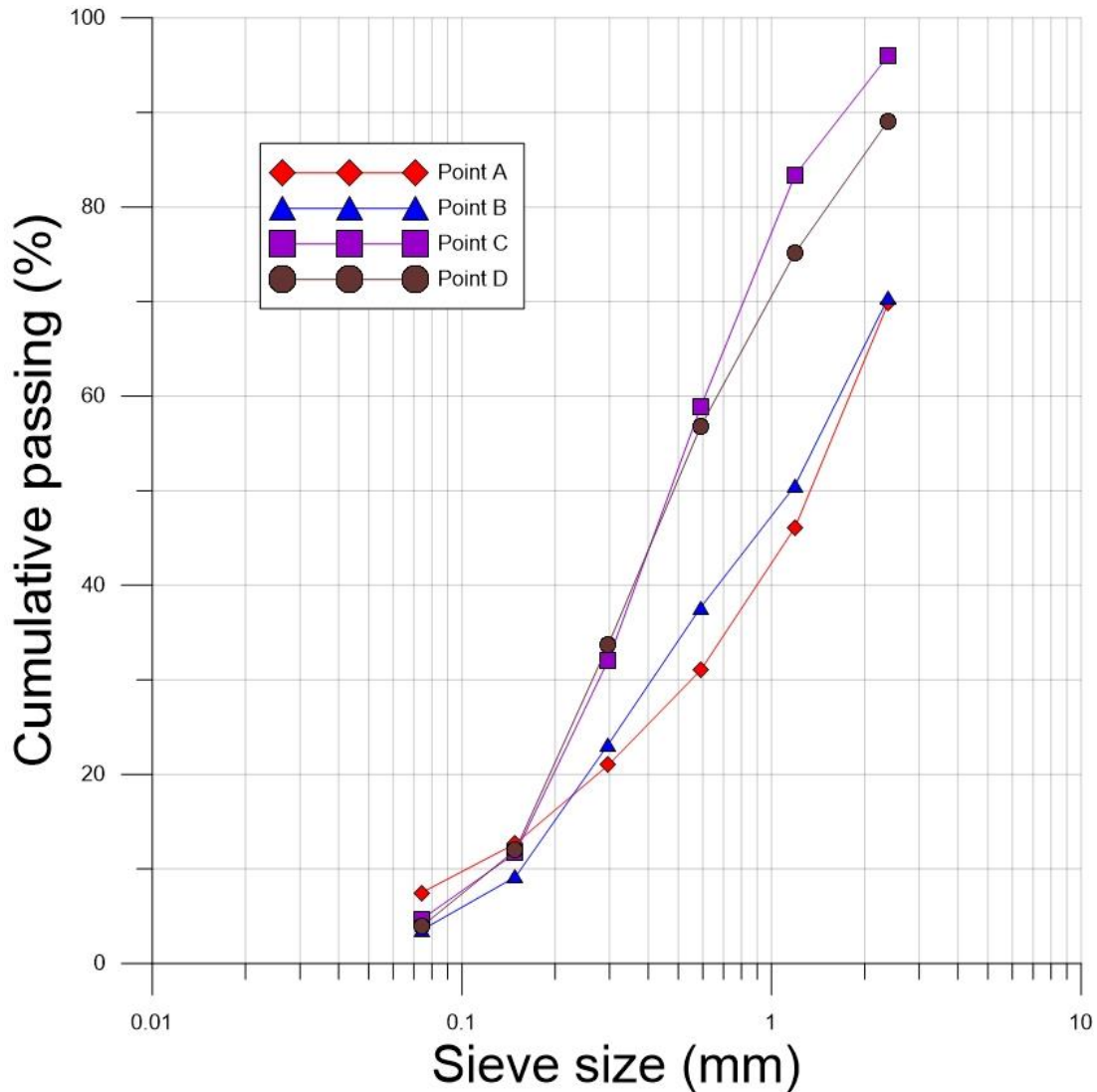


Figure 4-6: Particle size distribution curve

We used 4 methods to find out the soil particle type and mean diameter. They were the 1) Particle size distribution graph, 2) Soil texture triangle, 3) USDA soil size distribution chart, and 4) Fineness modulus of aggregate vs mean-diameter table. The type of soil can be determined by the soil texture triangle calculation. It was found out from the sieve analysis tables and graphs that most of the soil particles got retained in the sieves above 0.075 mm. Only less than 10 % of the whole soil samples passed through the no. 200 sieve as depicted in Table 8.

Table 8: Sieve collector pan retained percentage

Site points	A	B	C	D
Collector pan sample %	7.479	3.527	4.665	3.884

Therefore, when compared with the soil texture triangle, the soil used in this study was found to be sandy. As 90 % of the soil samples had already settled on the upper sieves, it means that these soil particles fall under the particle sizes of sand and gravel according to the values given by the USDA particle size distribution chart represented in Table 9.

Table 9: USDA particle size chart

Particle name	USDA (mm)
Gravel	> 2
Very Coarse Sand	1 - 2
Coarse Sand	0.5 - 1.0
Medium sand	0.25 - 0.50
Fine sand	0.10 - 0.25
Very fine sand	0.05 - 0.10
Silt	0.002 - 0.05
Clay	< 0.002

The diameter of the soil sample was then obtained using the fineness modulus vs soil particle diameter table. First the fineness modulus (FM) was calculated according to the formula –

$$FM = \frac{\sum(\text{cumulative \% residual rate})}{100} \quad (4.3)$$

These were the preliminary processes to calculate the mean diameter of the landslide soil. For the cumulative percentage residual rate summation, the percentage for 200 sieve number is excluded since that is only for clay. In our case, it is sand and gravel. The FM were calculated and the mean diameters were evaluated using FM and interpolation as shown in Table 10.

Table 10: Grain size distribution analysis results

Site points	Fineness modulus	Mean diameter (mm)
A	3.19	0.714
B	3.09	0.654
C	2.18	0.354
D	2.33	0.434

The mean diameters acquired were then compared to the USDA chart and the soil sample was finally concluded to be mixture of medium and coarse sand. The geotechnical parameters later assumed for simulation were based on this soil type i.e., medium & coarse sand.

4.2.4 COMSOL Multiphysics software

COMSOL Multiphysics is a modeling tool plus simulation platform that uses Finite Element Methods (FEMs) and Partial Differential Equations (PDEs) for solving various complicated scientific problems. The model creation is user-friendly and has physics-specified modules with good visualization properties. It

encompasses all the steps from model creation, defining governing equations, parameterization, and finally running the solver for analysis. The hydraulic properties can be added in the model using the Subsurface Flow Module and for the geotechnical properties the Solid Mechanics Module can be applied and then both of the modules can be coupled together and finally a user-defined hydro-mechanical model simulation can be executed. The mesh generation interface of COMSOL can generate a mesh with different densities according to the user specifications (Wei Shao et al, 2014). In COMSOL, the numerical solver used to predict the results is called MUMPS (Multifrontal massively parallel sparse direct solver). Its advantages are that it is a very fast solver saving time and memory. The only disadvantage is that it is sensitive to mesh quality. It is highly reliable and has excellent solving accuracy.

4.2.5 QGIS software

QGIS is a free and open-source multiplatform geographic information system (GIS) software application that allows users to view, edit and analyze geospatial data, in addition to composing and exporting graphical maps. QGIS supports both raster and vector layers. The vector data is stored as either a point, line, or polygon feature. It is a very handy software for extracting the elevation data from a geospatial image in very little time. All the data conversions from DTM data to an elevation text file in this research were obtained using QGIS.

4.3 Parameters and assumptions for Simulation

Proper determination of the controlling parameters needs to be done before the analysis. The slope geometry along with the initial groundwater level determine the initial safety factor. The rainfall characteristics and soil strength parameter changes worsen the stabilization leading to failure. Thus, attention is needed during

parameterization of these factors when dealing with rainfall-induced slope failures as they have a direct relation with it. The shear strength factors increase the safety factor of slope. More intensive rainfall increases the groundwater level rise (Zhang et al, 2011). The combined effect of groundwater level and water table level in subsurface flow was simulated using the COMSOL Multiphysics finite element software. The Subsurface Flow module of the COMSOL was used to describe the two-dimensional vertical and horizontal flow which was governed by the Darcy's law and Laplace's continuity equation. The Mohr-Coulomb failure criterion was used for the sliding soil mechanics. The Solid Mechanics module was used for the geotechnical part. Numerical analysis was performed to confirm the effects of these factors on landslide occurrence.

The cohesion, angle of friction and young's modulus were assumed according to the sieve analysis particle distribution results. The soil strength parameters of medium and coarse sand particles were used for this analysis. They were obtained from a geotechnical database available in the internet (Geotechdata, 2021). It was observed that there were soil descriptions similar to the current soil sample i.e., sandy gravel, medium sand or dense sands. The bedrock was taken as a sandstone since the topsoil consists mostly of sand and gravel and also referred from the Huisun area geology as mentioned in the literature review. Shale was not included in the bedrock layer for easier and faster simulation analysis. The parameters for sandstone were also assumed from the previous database. The parameters matching these type of soil particles were deduced and recorded as listed in the table no. 11.

Table 11: Geotechnical analysis framework

Analysis Parameters	Top soil (Medium & Coarse sand)	Sandstone	Water
Cohesion	0	-	-
Angle of friction	35°	-	-
Young's modulus	120 MPa (Megapascal)	26 GPa (Gigapascal)	-
Soil Density	2000 kg/m ³	2600 kg/m ³	1000 kg/m ³
Poisson's ratio	0.4	0.35	-
Porosity	0.5	-	-

The parameters present in the above table were used for the FEM simulation for slope stability. The bedrock was taken as sandstone according to the geology of Taiwan found in the literature (Ho, 1986; Tsou et al, 2011; Brown et al, 2012).

4.4 Initial & Boundary conditions

Before beginning the simulation processes, certain initial and boundary conditions were taken into account. The boundary conditions for the COMSOL hydrological and geotechnical analysis are divided into the initial conditions, the boundary pressure loads, the fixed and the free surfaces. The base and the vertical side of the slope model were kept as fixed so that the model domain itself doesn't move horizontally due to the boundary loads. The fixed constraint option in COMSOL was utilized for the fixing mechanism. The uneven sloping side was kept free to explore the slope failure. The graphical capabilities of the FE approach allow

a better understanding of failure mechanisms and simplifying the output from large datasets.

The soil was assumed to be permeable for pore water pressure formation. Selected areas of the slope were defined as a pressure boundary condition and the pore water pressure influence was checked. The phreatic line was obtained as a contour form and solid surface form according to the data provided. A boundary load was applied to the model which is the total water pressure affecting the vertical side of the model. The total water pressure includes the infiltration water and pore water-generated pressure. The boundary load was inserted using the pressure head, external load, and boundary load module of the COMSOL software.

For the initial conditions, the self-weight due to gravity was included using the gravity module and the soil parameters that govern the soil model stability were initialized by employing the Initial strain and stress module in COMSOL Multiphysics.

4.5 Procedure flow chart

The figure below shows the complete course of action taken for the simulation analysis.

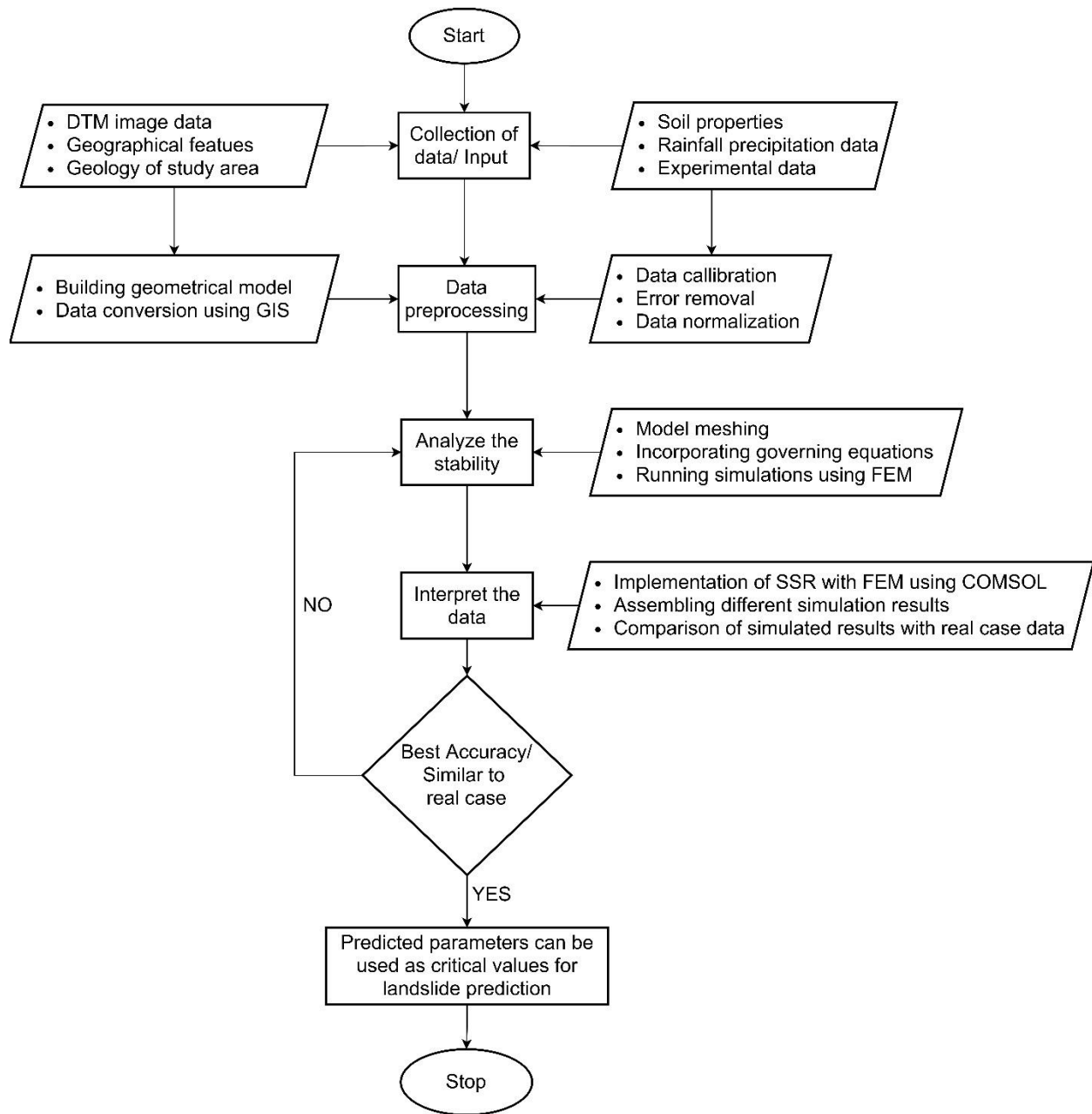


Figure 4-7: Course of action flow chart

The predicted results were compared to the real case which was the post landslide elevation data.

4.6 Gravity loading

The gravity weight is important in slope movements. For the application of gravity effects in a model, the gravity loading module is used. Forces are generated by the self-weight of the soil which is computed by a standard gravity procedure that involves integrals over each element, the equation being –

$$\mathbf{p}^{(e)} = \gamma \int_{vol} N^T d(vol) \quad (4.4)$$

Where N is the shape functions of the element and e is the element number. This equation estimates the area for each element and then multiplies it with the unit weight of soil and finally distributing the net vertical forces consistently to all the nodes. In the initial stress state, all the element loads are combined into a global gravity force vector and then applied to the FE mesh. The gravity loading can be defined in different ways according to the user. It can be equally distributed on a given area, or it can be applied at a single point to make a stress-free model. In elastic condition models, sequential loading is used where the gravity is incremented to cause deformations but not stresses. The parameter unit weight assigned to the soil is directly proportional to the nodal self-weight loads generated by the FEM model due to gravity.

Chapter 5 Results & Discussion

5.1 Preprocessing and Data Conversion

The image data of the study area were aerial photographs, which was obtained from the Aerial Survey Office, Forestry Bureau, Council of Agriculture, Executive Yuan, Taiwan. It was first accessed using QGIS software. Four image data for different years i.e., 2007, 2009, 2013, 2018 were studied. The 2007 image was sized 20×20 (m) while the 2009, 2013 and 2018 image were sized 0.25×0.25 (m). The shapefile option was used to create a polygon to trace the landslide area out of the whole map. A line was drawn at the middle of the polygon from its top to bottom using the multiline function. After the line was created, 52 points were marked on the line with equivalent space distance for acquiring the coordinate and elevation points. All the distance and station calculations were done in excel. After obtaining the stations, they were marked on the map for every 200 m elevations to get a better visualization and understanding of the elevation of the study map. Fig. 5-1, 5-2 and 5-3 represents the 4 different year's corresponding maps.

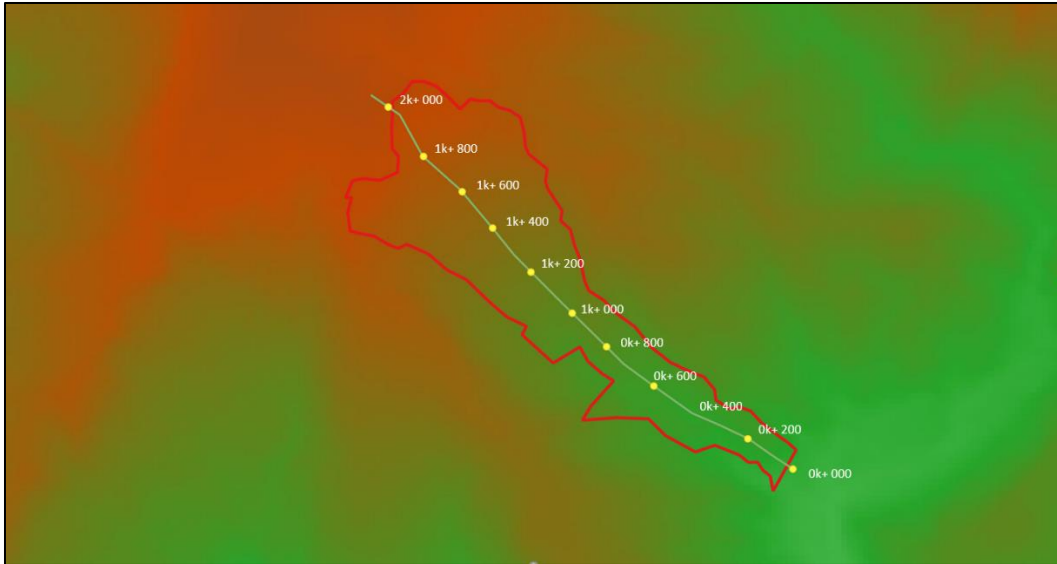


Figure 5-1: 2007 DTM data

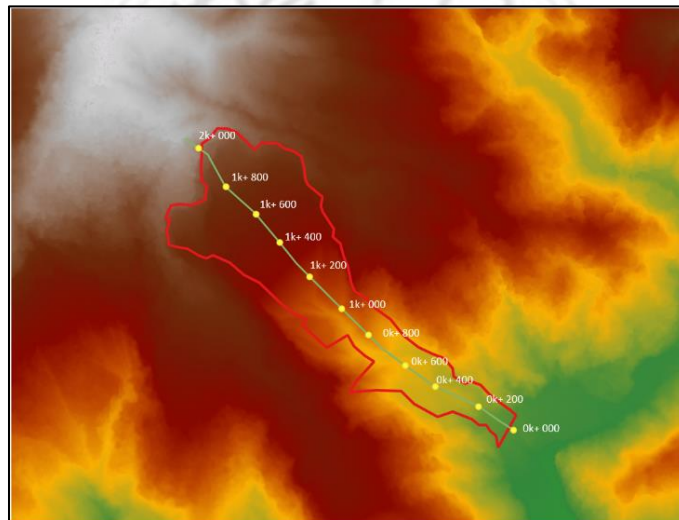


Figure 5-2: 2009 DTM data

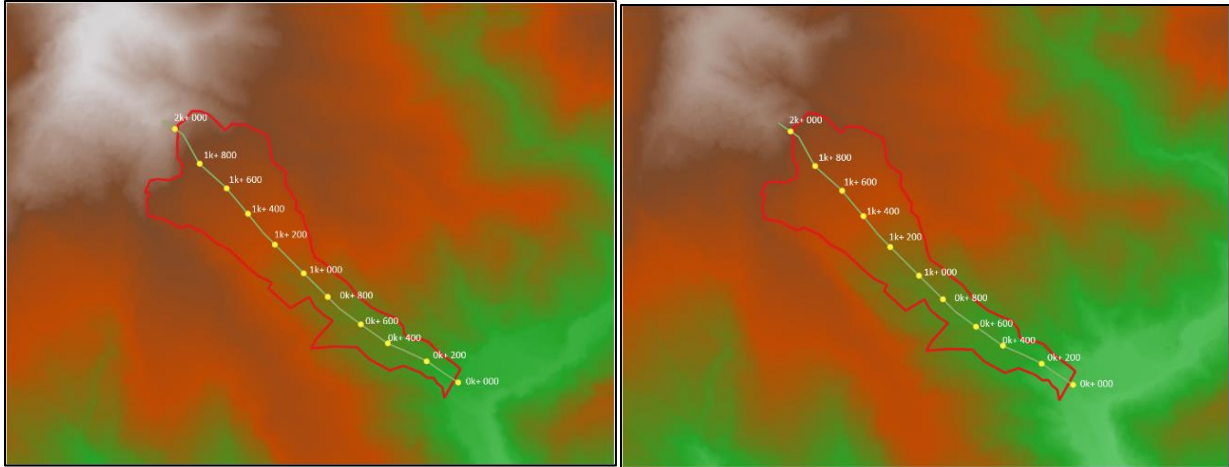
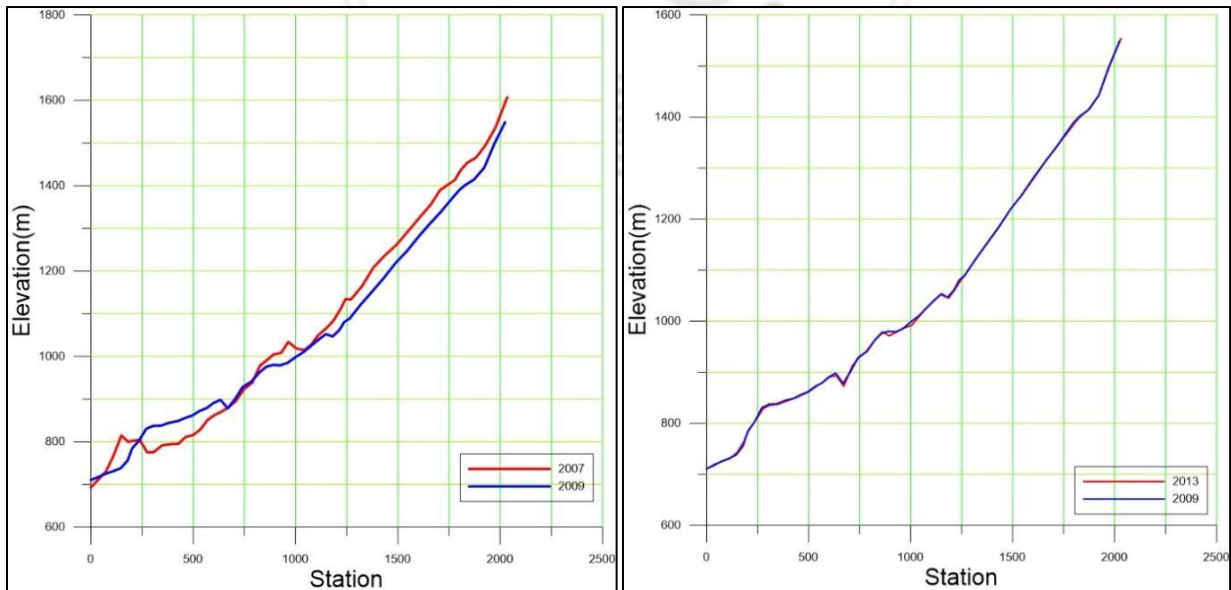


Figure 5-3: 2013 & 2018 DTM data

After the map markings, graphs were plotted between the elevation and station values to compare the four-elevation data and observe the landslide movements and structure of failure i.e., Fig. 5-4. The x-axis is the elevation while the y-axis shows the stations.



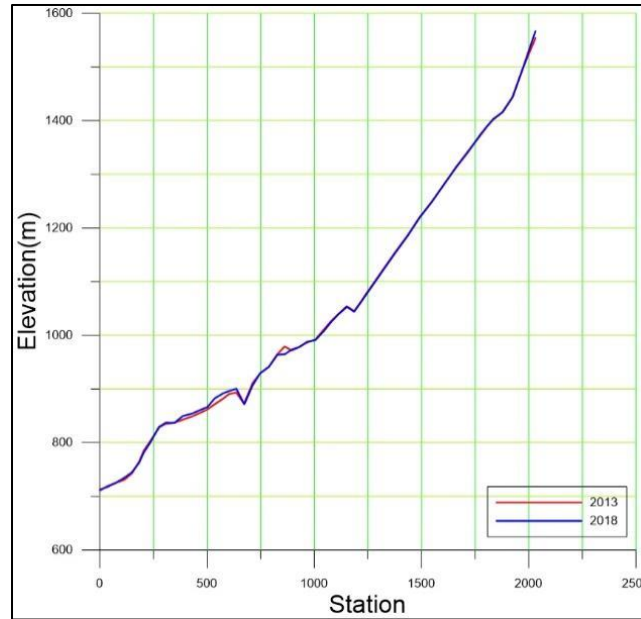


Figure 5-4: Elevation difference graph between different years

The first graph shows the elevation of the slope side for 2007 and 2009. A large change has been noticed in the graph which reveals the occurrence of a landslide between the 2 years. For the other 2 graphs, only little elevation changes have been observed proving no landslide has occurred during the periods. The minute elevation changes may be due to some weathering of rocks or some small debris movements on the slope surface soil due to gravity or climatic events. These small elevation changes are common as the upper surface soil is exposed to the environment. This exposure leads to soil erosion and weathering as a result of rainfall, storms, snowmelt, aging, and tectonic movements. It may sometimes lead to reactivation of the landslide area.

5.2 Numerical Model Creation

The slope stability analysis and the numerical simulation of the slope model were done by the Finite Element Method (FEM) using COMSOL Multiphysics

software. First, the elevation data was extracted from the study area Digital Terrain Model (DTM) map using QGIS software which uses geographical information system. Then the elevation data was imported into the FEM analysis software to create the geometry model for the simulation analysis. The model geometry was modeled with basic soil properties representative of Mohr-coulomb plasticity coupled with Darcy's law subsurface flow analysis. In this study, a 2-D geometry layout was first designed which was later converted to a solid model for analysis. The FEM simulations were conducted on the slope model and its respective landslide failure movements were recorded. The model was derived from the elevation data extracted from the 2007 DTM map shown in Fig. 5-5.

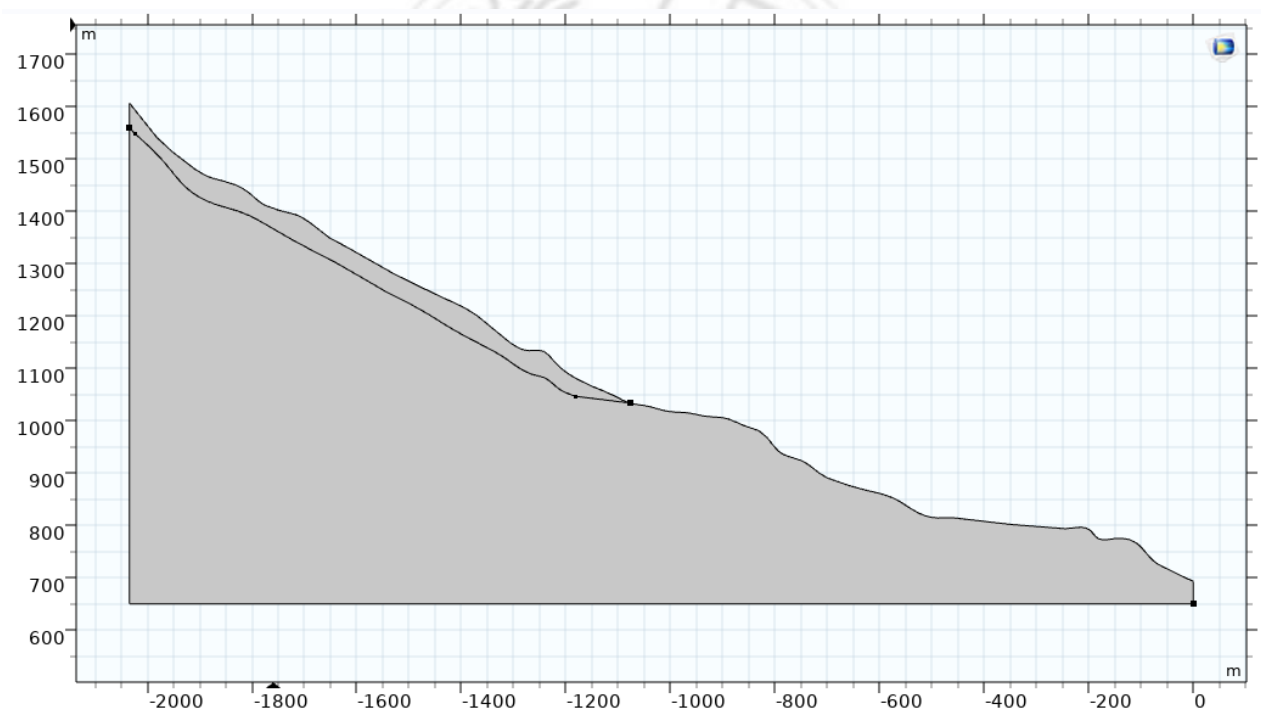


Figure 5-5: Model geometry

The elevation data was imported from excel to COMSOL to model the irregular slope of the Huisun Forest area. The process involves importing the elevation file, then creating a parametric surface, and then uniting the whole surface

with a solid function so that computational analysis can be done on the model as a whole single body or domain in FEA terms. An impervious boundary was applied at the contact between the soil cover and the bedrock. The Multiphysics model was kept simple, consisting of topsoil and bedrock. The topsoil consists of soil, sand, gravel, and weathered rocks. The thickness of topsoil was about 60 - 70 meters while the bedrock lies below the topsoil layer starting at the depth of 70 meters.

5.3 Meshing of the Model

The accuracy given by the FEA is mostly due to its meshing analysis. When a mesh is created, it splits the domain into a discrete number of elements for which the solution is evaluated. These elements can be of different shapes and have nodes for connecting with other elements. When a load is applied in a mesh body, the forces are transferred through the nodes of the elements. There are different types of solid elements depending on their shape. Triangles and quadrilaterals for 2-D mesh and tetrahedral, pyramid, or hexahedral for 3-D meshing. Every shape has its own advantages and disadvantages. In this study, the triangular shape elements have been used for mesh creation in FEM analysis. This cell shape consists of 3 sides and is one of the simplest types of mesh. The triangular element has 3 nodes. When a model changes its shape due to any external forces, the nodes exhibit vector movement with nodal displacements.

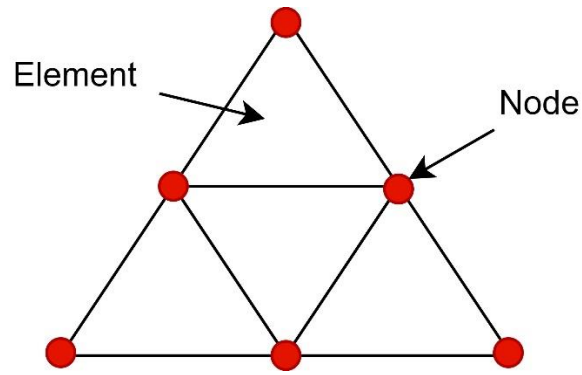


Figure 5-6: Two-dimensional linear triangular elements diagram

When a continuous object is analyzed, it generally has infinite DOFs. This DOFs make the analysis more difficult as it creates many conditions and convergence of solutions cannot be reached. Thus, with the use of mesh, the DOF can be reduced and the analysis becomes finite and fast. The mesh discretizes the stress gradients precisely.

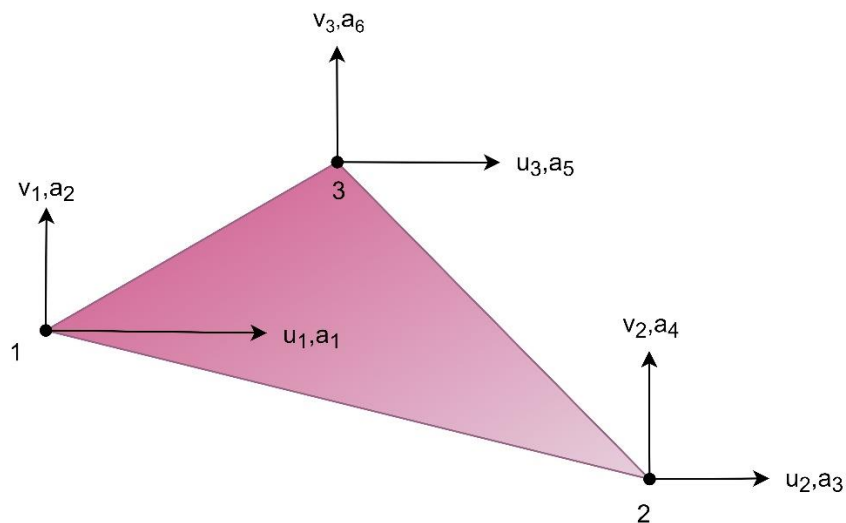


Figure 5- 7: Nodal displacement for triangular element

Where $a_1, a_2, a_3, a_4, a_5, a_6$ are the vectors associated with the u and v nodal displacements. A triangular surface mesh is always quick and easy to create. The advantage of triangular meshing is that it reduces the time for simulation analysis and gives better accuracy since a triangle shape can cover more voids in an irregular or complex geometrical structure. i.e a landslide structure as it has no fixed geometric shape.

The element size is very important in meshing analyses. Big elements and coarse meshes will give more errors. Smaller the mesh size, the better the results due to better sampling across physical domains but significant increase in the computational time. Reducing the element size helps in obtaining results with better accuracy. It is always advised to add more elements near the failure or deformation areas for saving computational time and getting satisfactory results as done in this case. A balance between the accuracy and computing time should be checked. In this research, the mesh called the Extra fine mesh was used in COMSOL for superior results. In this simulation, the soil was treated as a porous medium in a solid phase. The element size is very important in meshing analyses. Big elements and coarse meshes will give more errors. Smaller the mesh size, the better the results due to better sampling across physical domains but significant increase in the computational time. Reducing the element size helps in obtaining results with better accuracy. It is always advised to add more elements near the failure or deformation areas for saving computational time and getting satisfactory results as done in this case. A balance between the accuracy and computing time should be checked. In this research, the mesh called the Extra fine mesh was used in COMSOL for superior results. In this simulation, the soil was treated as a porous medium in a solid phase.

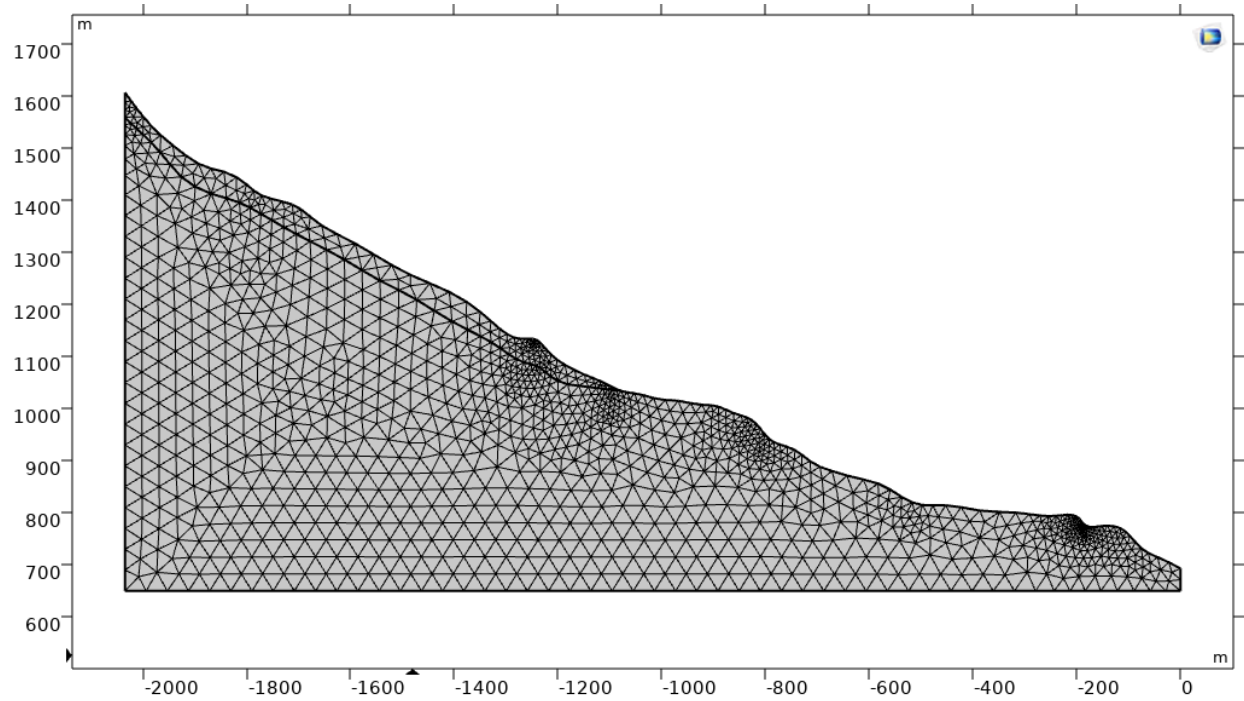


Figure 5-8: Model meshing

The extra-fine mesh analysis used in FEM is good for slope analysis. There were approximately 2800 triangular elements present inside the mesh. The triangular elements are equilateral and the element size ranged from 5 meters to 42 meters. The smaller elements were present at the deformation and failure zone areas while the other rigid bedrock parts of the slope model were comprised of bigger element size up to 42 meters. The element size near the Some of the elements were used to mesh the soil while the rest for rock meshing. The two meshes were different as the overlying soil will show more movement and plastic behavior while the bedrock layer was kept as a rigid material that will not have no displacements.

5.4 Slope Stability Analysis

5.4.1 Subsurface Flow Analysis

A slope stability analysis is mainly composed of a hydrological and geotechnical analysis. The water movement, solute transference, and complicated pore structures can change the prediction results drastically and on the other hand, they are difficult to direct in the analysis system. Therefore, the subsurface flows that occur inside the soil play an important factor in the failure of landslides. The various flows occur through the macropores, fissures, pipes, fractures, etc., and have no specific direction or formation (Wei Shao et al, 2014). For this analysis, first, the slope model was created and then the hydrological features were added to create the required environment. The hydrological features include the groundwater level, water table pressure, pore pressure, seepage, and boundary pressure of the water body. These factors were combined and induced in the model and the consequent effects were examined. The combined effect of groundwater level and water table level in subsurface flow was simulated using the COMSOL Multiphysics finite element software. The Subsurface Flow module of the COMSOL was used to describe the two-dimensional vertical and horizontal flow by Darcy's law equation. This module can be used for the numerical inspection of geophysical and environmental happenings related to subsurface flows.

Darcy's law interface comes under the Subsurface flow module which is mostly used for stationery and time-dependent analyses. This is a physical interface that does fluid flow simulations based on permeability, porosity, and frictional resistance between pores where the pressure gradient/head is the major driving force and the velocity of fluid flow inside the model is low. The pressure head contours and pressure surface plots were based on Darcy's law. The net flux across a face of

a porous surface (COMSOL Multiphysics Reference Manual, 2018) according to Darcy's law is –

$$u = -\frac{\kappa}{\mu}(\nabla p + \rho g) \quad (5.1)$$

And the continuity equation used to represent the fluid dynamics was –

$$\frac{\partial}{\partial t}(\rho \varepsilon) + \nabla(\rho u) = Q_m \quad (5.2)$$

Where u is the flow velocity (m/s), κ is the permeability of the porous medium (m^2), μ is the dynamic viscosity of fluid, ε is the porosity, p is the fluid pressure (Pa), Q_m is the mass source term ($\text{kg}/\text{m}^3\text{s}$) and ρ as the density of the fluid (kg/m^3). The Fluid and Matrix properties node beneath the Darcy's law interface is used to add the governing equations related to fluid dynamics which combines the Darcy's law with the continuity equation that is -

$$\frac{\partial}{\partial t}(\rho \varepsilon) + \nabla \rho \left(-\frac{\kappa}{\mu}(\nabla p + \rho g) \right) = Q_m \quad (5.3)$$

First, the initial values for the respective pressures are added to create an initial condition for the ephemeral simulation and act as a starting point for the analysis solver. The gravity forces were also added for better accuracy of the analysis. The gravity forces are automatically distributed on the selected domain according to the elevation of the slope structure. Finally, the pressure head is applied using the fluid interface which drives the fluid movement inside the porous model, developing a flow line. The pressure is calculated by-

$$p = \rho g H \quad (5.4)$$

Where g is the acceleration due to gravity and H is the height of the water body. The pressure head is created by combining water pressure load oppressing the

top of the slope surface due to rainfall and the elevation potential from the start to the end of the flow lines. The No Flow node can be used to make some required areas impervious. It is a boundary condition to break off all fluid flows for some specific boundaries which represent the non-porous areas around the slope model and also to reduce the analysis processing time, for example, the base of the hillslope.

After every factor and condition is applied and the simulation environment is created, the stationary solver with physics-controlled settings is started and the simulation takes place. At the end of the simulation, the pressure on different areas of the domain and the flow lines are computed. The flow lines are observed using the contour feature of the pressure head node. These flow/phreatic lines represent the seepage lines, which show the direction and path for how the water from the surface of the soil will seep through the soil and come out from the downstream side. Portrayals of the critical groundwater line can be built from these seepage lines. After the subsurface fluid analysis is completed, the results and the resulting model are further used for the second phase which is the solid mechanical analysis.

5.4.2 Geo-mechanical Analysis

This part of the research deals with how the soil surface will deal with the hydrological factor impacts. The Mohr-Coulomb model, Brook's Corey model, van Genuchten model, etc. belongs to the group of geotechnical analysis methods. The Mohr-Coulomb failure criterion was employed in the sliding soil mechanics in this study. The Solid Mechanics module was used for the geotechnical processes. The application of stresses and forces related to geotechnical analysis is done in this part. The Solid Mechanics interface comes under the Structural Analysis module of COMSOL. It can conduct nonlinear analyses for two-dimensional, three-dimensional, and asymmetric bodies. In our study, we have used a 2D model for the stress, strain, slippage, and displacement analysis. For geomechanical analysis for

soil bodies, there are 5 main models mostly used i.e., Cam-Clay, Drucker-Prager, Mohr-Coulomb, Matsuoka-Nakai, and Lade-Duncan models. All have different analysis calculations with divergent parameters used. A series of equations of motion are solved together on a solid selected model and results such as stresses, strains, displacements, and other coefficients were computed. This interface allows the addition of material type and other geological parameters making the model act as a real-life soil structure and therefore the results will be more real. The initial stresses were applied to the model and the effective stress and strains were investigated at the end from the numerical simulation results. The stress and strains acting inside the FEM model was described using the following symmetric stress α and strain ε tensor matrix equations–

$$\alpha = \begin{bmatrix} \alpha_x & \tau_{xy} & \tau_{xz} \\ \tau_{yx} & \alpha_y & \tau_{yz} \\ \tau_{zx} & \tau_{zy} & \alpha_z \end{bmatrix} \quad (5.5a)$$

$$\varepsilon = \begin{bmatrix} \varepsilon_x & \varepsilon_{xy} & \varepsilon_{xz} \\ \varepsilon_{xy} & \varepsilon_y & \varepsilon_{yz} \\ \varepsilon_{xz} & \varepsilon_{yz} & \varepsilon_z \end{bmatrix} \quad (5.5b)$$

Where $(\alpha_x, \alpha_y, \alpha_z)$ and $(\varepsilon_x, \varepsilon_y, \varepsilon_z)$ are the normal stresses and strains acting on the 3 coordinate directions. $(\tau_{xy}, \tau_{xz}, \tau_{yx}, \tau_{yz}, \tau_{zx}, \tau_{zy})$ and $(\varepsilon_{xy}, \varepsilon_{xz}, \varepsilon_{yx}, \varepsilon_{yz}, \varepsilon_{zx}, \varepsilon_{zy})$ are the shear stresses and strains acting on x, y and, z directions on the model framework. Due to the symmetrical analysis, the shear stresses acting on the opposite sides are taken equal i.e., $\tau_{xy} = \tau_{yx}, \tau_{xz} = \tau_{zx}, \tau_{yz} = \tau_{zy}$. The evaluation was done using the default Linear Elastic Material which adds all the equations related to a linear elastic model and extends the application of geological parameters like stresses, plasticity and, boundary loads. The Young's modulus (E), Poisson's ratio (ν), and density of the material were included in the analysis model representing the elastic material properties. The elastic constant

equation relating the 3 moduli where one is user-defined while the other two are calculated by default i.e., the default Bulk modulus (k) and Shear modulus (G) is -

$$E = \frac{9kG}{3k + G} \quad (5.6)$$

The equation of Poisson's ratio in terms of Bulk modulus and shear modulus is -

$$v = \frac{1}{2} \left(1 - \frac{3G}{3k + G} \right) \quad (5.7)$$

The current model was chosen as isotropic which means that the material will have same properties in all sides. Since for the stress and slippage analysis were done in 2D, plane strain assumptions were used. The Mohr-coulomb yield criterion was selected for the soil plasticity analysis which takes the cohesion (c) and angle of friction (Φ) parameters in account. The c and Φ values were entered according to the study area soil size analysis and the simulation process was begun. FEM uses matrix calculations and, in this case, the material stiffness matrix M was engaged (COMSOL Multiphysics Reference Manual, 2018) and is shown as -

$$M = \frac{E}{(1 + \nu)(1 - 2\nu)} \begin{bmatrix} 1 - \nu & \nu & \nu & 0 & 0 & 0 \\ \nu & 1 - \nu & \nu & 0 & 0 & 0 \\ \nu & \nu & 1 - \nu & 0 & 0 & 0 \\ 0 & 0 & 0 & \frac{1 - 2\nu}{2} & 0 & 0 \\ 0 & 0 & 0 & 0 & \frac{1 - 2\nu}{2} & 0 \\ 0 & 0 & 0 & 0 & 0 & \frac{1 - 2\nu}{2} \end{bmatrix} \quad (5.8)$$

The equations involved in this matrix are shown at elastic properties and constants in Chapter 3 of this research. The soil model was considered isotropic for this research case i.e., the properties of the linear elastic body will remain alike for

every direction. Initial stress values were added to the model to serve as an initial condition for the transient simulation afterward. Adjusting the initial values before starting the simulation, results in faster and accurate failure analysis since the analysis will start directly from the initial stage values (i.e., not starting from zero stress) saving a lot of computational time and complexities. The initial strains were kept as zero as they will directly change with the initial stresses induced. After the addition of the initial values, the loads and constricts were affixed to the model. The top of the slope was subjected to a boundary load and the external stress node was used for adding them. It specifies an additional stress contribution which an external force distribution and not related to the internal equation constitutive model. In our case, it's the pore pressure load. The calculation of the pore pressure load is dependent on two parameters 1) absolute pressure and 2) Biot-Willis coefficient. The absolute pressure is user-defined while the Biot-Willis coefficient is taken as 1.

In the model, some areas need to stay rigid so that the whole domain doesn't get displaced due to an external load. The base of the landslide model was made fully constrained which makes the displacements and rotations of that area equal to zero in all directions. In default, all the areas and edges of the model are considered free (no boundary conditions applied). Hence, when some areas are constrained, the other parts will stay free and work similarly to a real geological structure. The gravity condition is added in this solid analysis which is similar to the subsurface flow analysis. The default condition is g_const having a constant value of 9.8066 m/s^2 .

5.4.3 Coupled Hydro-Geo-mechanical Simulation

The kinematics of the slope play a vital role in SSA as it changes variably with many factors like soil strength properties, slope geometry, geological conditions like the soil type and bedrock conditions, and water table fluctuations. Deep-seated landslides with clayey materials encounter rotational failures while

some shallow or deep landslides which occur in overlying bedrock weathered rocks manifest the infinite slope failure. When doing numerical analyses with such conditions it is important to evaluate it using coupled multiphysics analysis, assuming the known kinematics. The coupled FE analyses involving different geotechnical parameters provide an excellent framework for evaluating slope stability and also prediction of the groundwater fluctuation range (Leshchinsky et al, 2015).

In traditional slope stability analyses, only a single hydrological analysis is conducted, where the rainfall influences are incorporated by changing the groundwater flow patterns with increasing pressure heads or rising groundwater tables. But a landslide is not only dependent on the hydrological factors but the geotechnical factors play a vital role too. That is why in this research, a modern analysis was done where two analyses were coupled together using the shear strength reduction method and finite element. The reduction of shear strength factors plays a critical role in destabilization. Escalation of pore water pressure and seepage forces generally lead to rainfall-induced landslides in natural slopes. It has been found that positive pore pressures build up along the soil/bedrock interface or the low area of the slope which initiates movement. This develops weakening along the sliding surface and movements become more rapid leading to failure of the slope. The sudden acceleration of the failed mass is caused due to formation of continuous shear surface and rapid generation of large plastic strains.

Coupling subsurface flow analysis with elastoplastic geo-mechanical analysis (Solid mechanics) is an example of the Multiphysics analysis. It involves predefined multiphysics couplings and conditions. The FE modeling was carried out in steady-state conditions. The soil is taken as homogenous sandy soils. When the required model simulation environment is created, the simulation is started where the system

will automatically induce the pore pressures and shear stresses incrementally and thus reaching the failure point. Five analyses were done after coupling the 2 studies i.e., subsurface and geotechnical mechanics. The simulation results done were 1) Flowlines, 2) Pressure distribution, 3) Von-mises stress, 4) Effective plastic strain and 5) slope displacement. In every analysis the red zone represents the maximum affected areas whereas the blue depict vice versa. The pressure head analysis simulations found out the seepage flow lines of the landslide slope with the pressure distribution as shown in fig. 5.9 and fig 5.10.

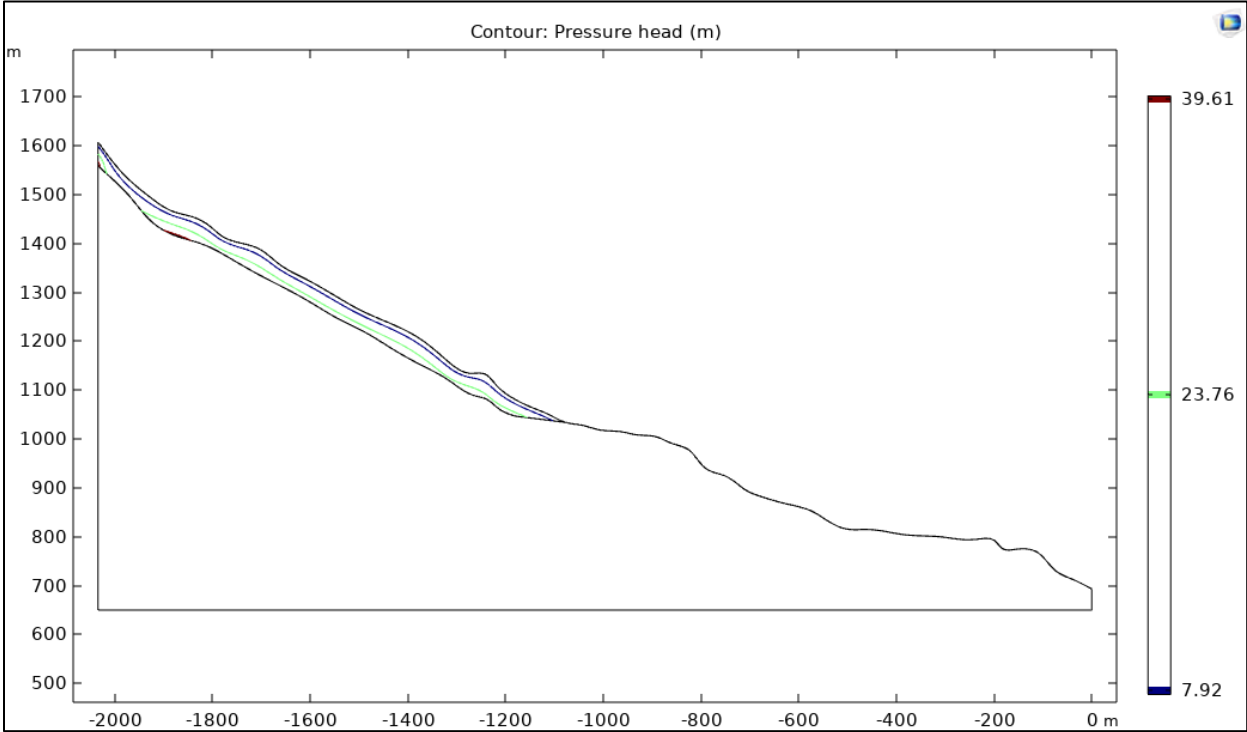


Figure 5-9: Pressure head analysis result

The boundary conditions for the COMSOL hydrological and geotechnical analysis are divided into the initial conditions, the boundary pressure loads, the fixed and the free surfaces. Selected areas of the slope were defined as a pressure boundary condition and the pore water pressure influence was checked. The pressure-head

flow lines obtained from the analysis show the flow lines the water will seep through the soil body and then come out from the other side which is the base of the mountain causing seepage erosion and finally will cause landslide at some point when the soil surface is at its weakest. The critical groundwater range can be extracted from these flow lines which can mark the water level in the mountain slope. The critical groundwater level from the base of the sandstone rock layer ranged from 7.92 m to 39.61 m. The figure shows the variation of GWL in the slope. It can be seen that it increases with depth. The GWL near the slope surface is very low. Piping occurs in these flow lines due to seepage and pore water pressures. These pipes once formed, become larger with time due to the runoff tendency of water. Finally, the water traveling through the pipe emerges from the natural slope surface, representing the discharge area. It is at this moment that marks the most vulnerable point of the slope surface. When the slope finally loses all its stress resistance, the stability fails and the soil mass will collapse.

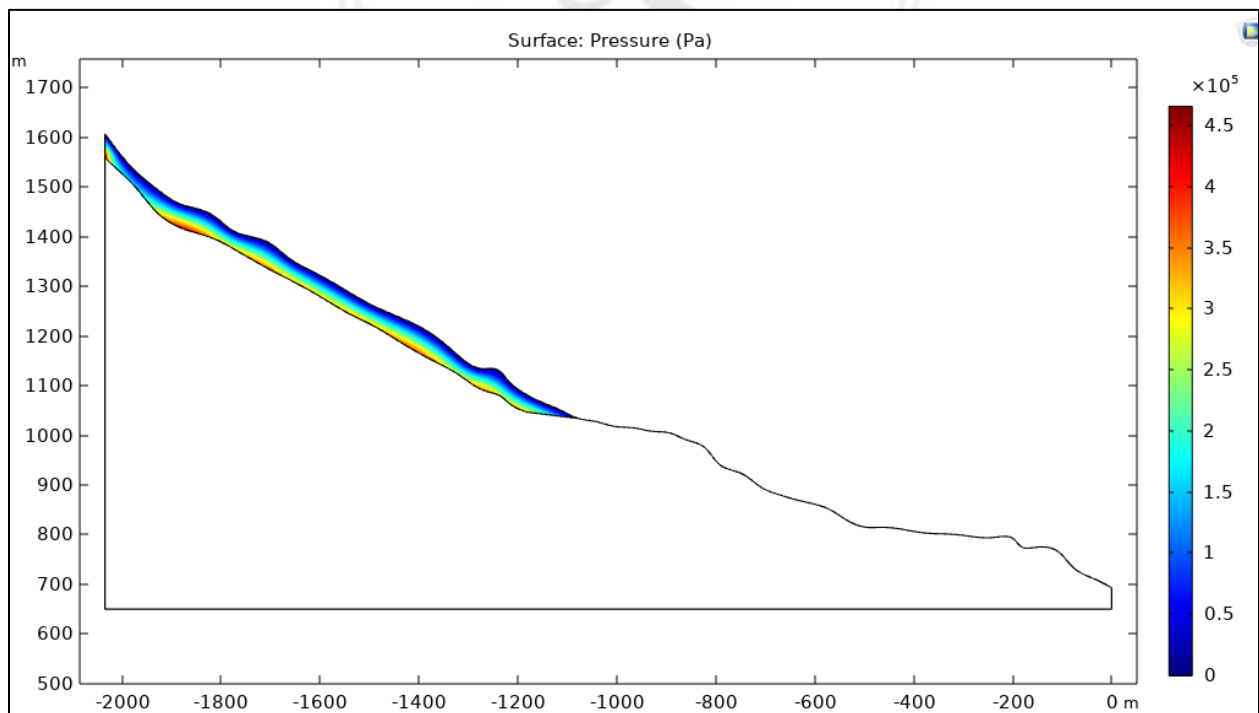


Figure 5-10: Pressure analysis result

The von-mises analysis simulations showed the effective stresses and forces affecting the slope during failure. The stresses went up to 5.4 MPa represented by the red regions. If a landslide mass is moving along the sliding surface, the measured displacement rates are likely to be higher for weaker sliding surfaces. The relation between the displacement and strength parameters is important. It was observed that there was huge stress formed at the interface of the soil layer and bedrock. This is due to the sliding shear movement of the soil layer over the bedrock during failure. It will put high stress on the soil-bedrock interface. The other stresses in the bottom and the left side are neglected as they are formed due to the fixed boundary conditions inserted in the model during creation for analysis and is not related to the study.

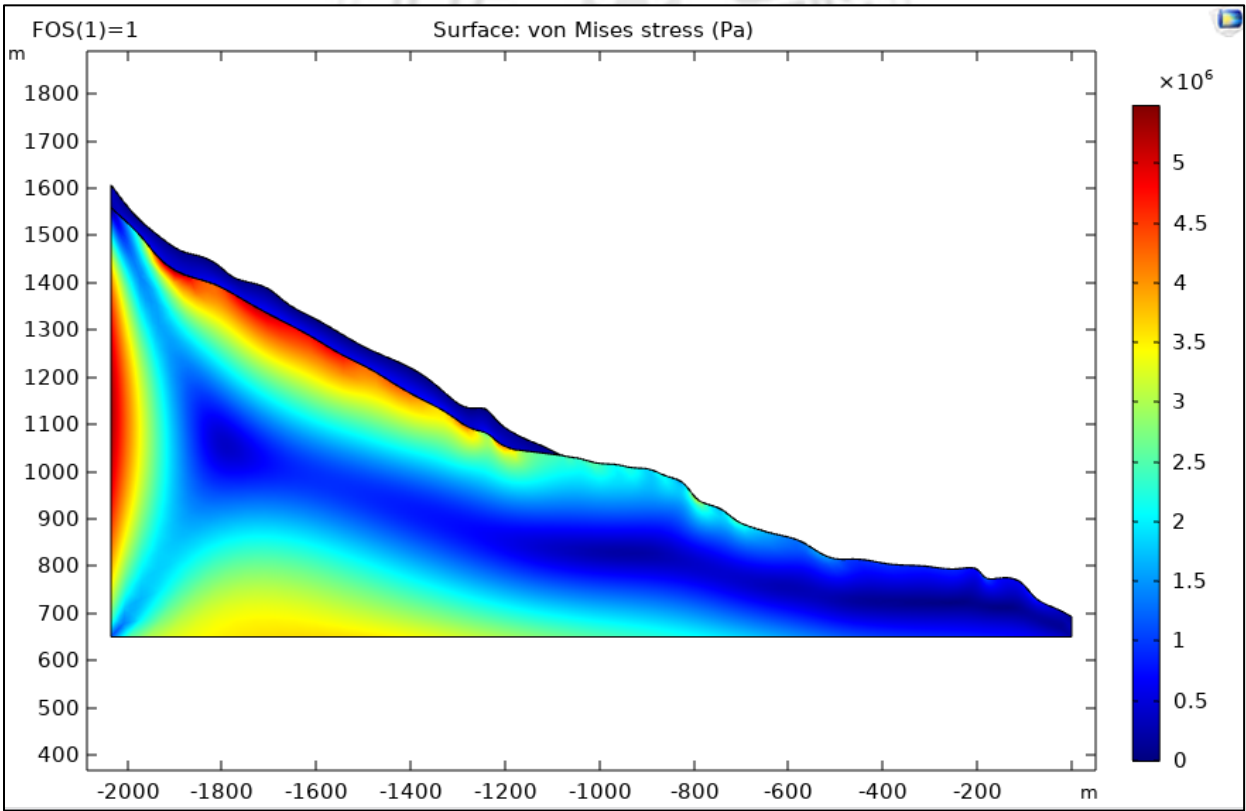


Figure 5-11: Von-mises stress analysis result

The FOS was gradually increased until the convergence fails within the iteration limit. The FOS was initially taken as 1. It was observed that when the FOS reached 1, there was a sudden increase in the displacement. This marks the failure point where the algorithms are unable to converge and we get the required result. After the typhoon rainfall event, the groundwater level increased, which increased the pore water pressures inside the soil leading to seepages. The pore water and seepage pressures rising, gradually decreased the shear stress of the soil body and finally, the landslide occurs when topsoil could not hold itself anymore causing displacement of the soil mass downstream. From the results, it was found that the groundwater level was located above the bedrock. The critical slip surface is developed on the soil-bedrock interface after the hydro-geotechnical analysis, which shows good agreement with the actual failure zone, as shown in the elevation graphs. The simulated results have illustrated that the methodology applied in this work is consistent with deep-seated rainfall-induced landslides. Then comes the effective strain analysis which reveals the region where the strains will be highest along the slope surface. The negative value indicates that the slope has undergone compressive stress effects. These strains gave rise to the displacements that occurred during the landslide.

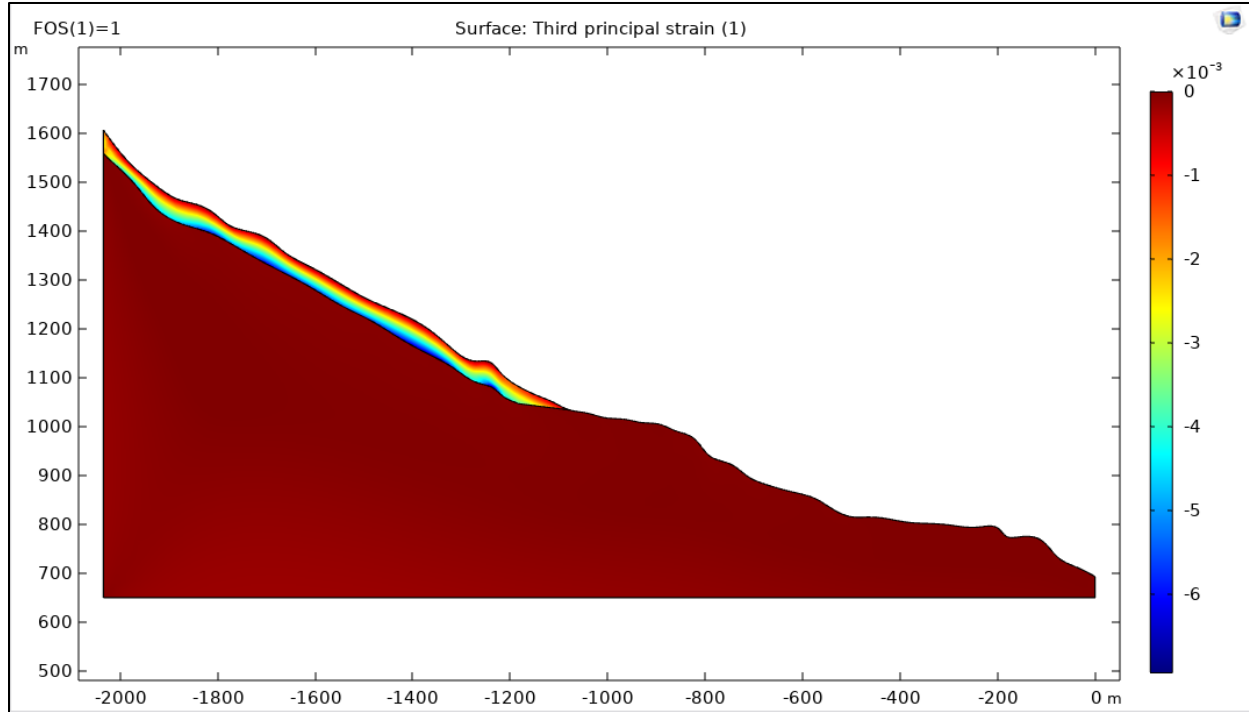


Figure 5- 12: Effective strain analysis result

The measured landslide displacement was reproduced numerically through the use of FEM with a coupled two-dimensional hydro-mechanical analysis. The model recorded the horizontal displacements within the finite element mesh, demonstrating reasonable agreement. As implied from the displacement results, the movement was mostly parallel to that of the bedrock thus implicating a translational infinite slope failure. This is an important analysis as it shows the landslide zone which is going to slide down the slope surface. The equation used by the system to find a dimensionless displacement D is:

$$D = \frac{E' \delta_{max}}{\gamma H^2} \quad (5.9)$$

Where, δ_{max} is the maximum nodal displacement at convergence and H is the height of slope.

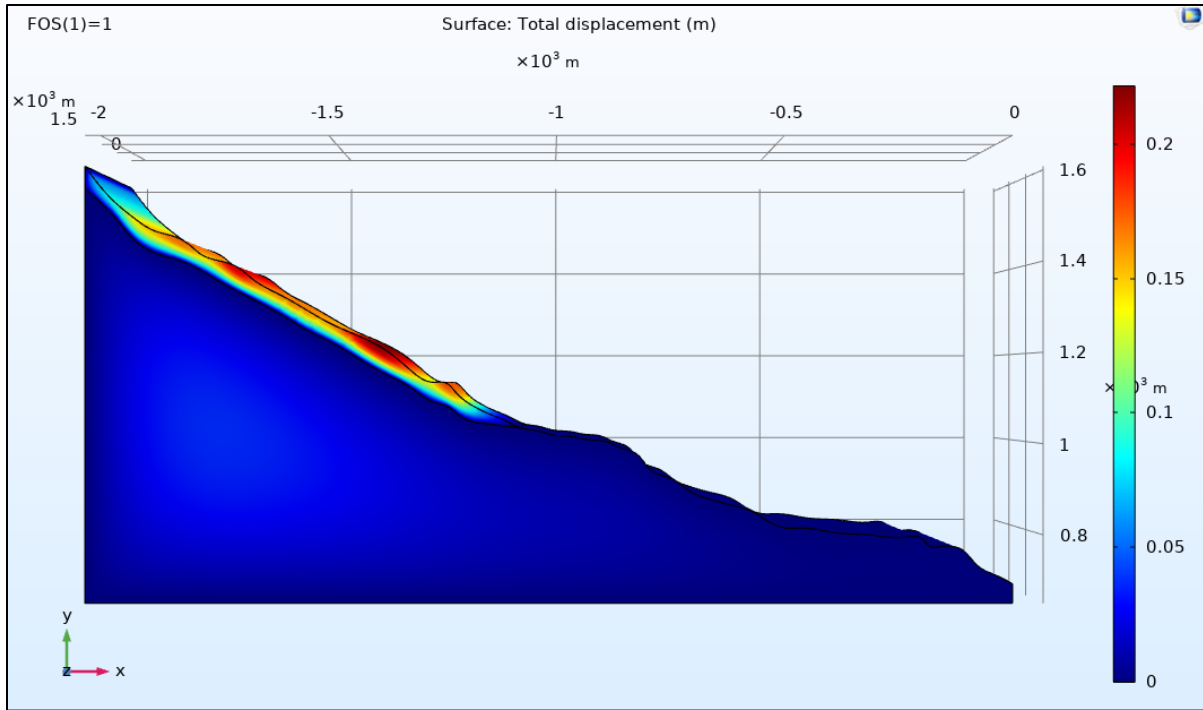


Figure 5- 13: Total displacement analysis result

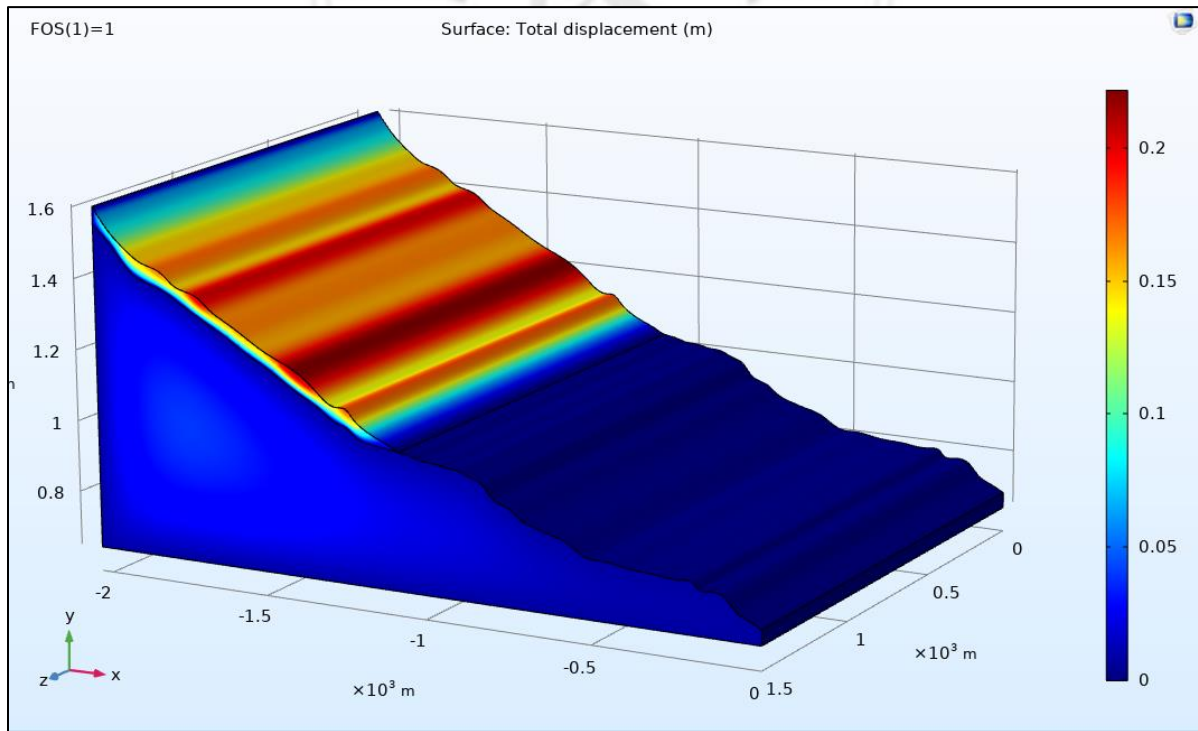


Figure 5- 14: 2-D Extrusion model of slope displacement

The displacement analysis estimated that the maximum displacement was about 224 m long. The displacement analysis results have shown successful agreement with the original landslide data. The measured landslide displacement was reproduced numerically through the use of FEM with a coupled two-dimensional hydro-mechanical analysis. The results acquired from the all the simulation analyses for FOS 1 are tabulated in Table 12.

Table 12: Simulation predictions

Simulated output parameters	Predicted values/range
Pressure head (PH)	7.92 – 39.61 (m)
CGWL (from PH range)	23.76 m (most probable)
Maximum pressure	4.7×10^5 Pa
Max. effective stress	5.4×10^6 Pa
Effective strain (minor principal)	-6.88×10^{-3} (compressive)
Maximum displacement	≤ 224 m

In this type of hydro-mechanical analysis, the slope is considered completely saturated when the flow lines attained from the process coincide with the slope surface. The combination of Darcy’s law and continuity equation was considered to be the most robust method for performing hydraulic analysis. During traditional computational analyses, serious limitations impose restrictions on the model. This is not the case with numerical analysis. The advantage of using numerical analysis is that it can integrate more sophisticated and advanced models of soil hydraulic and

geotechnical properties. The deformation of the slope was observed and displacement and GWL values were recorded.

5.5 Significance of this research

Storm-induced landslides are frequent in tropical and sub-tropical climate regions like Taiwan, Japan, India, etc. The proposed method is capable of pre-analyzing the slope stability of landslide zone slopes. The displacement analysis results have shown successful agreement with the original landslide data. The presented case study described the translational failure displacement and slope stability of a rainfall-induced landslide in the Huisun forest area, Nantou, Taiwan after analyzing through a numerical model. The FEA captured the destabilization and failure of the slope with the help of a rainfall-enabled calibration and various hydraulic and geotechnical parameters. The numerical model employed SSR techniques to increase the accuracy of stress action and FOS in the model. The water table fluctuations and high rainfall amount resulted in rising instability among the slope surfaces. Many kinds of research have been done in this field but the effect of pore pressure and shear strength of soil has not been included which has a huge impact on these landslide activities.

When using a computer-assisted simulation wielding FEM it is important to input appropriate parameters for analysis and the system must have an accurate judgment and credence in its usability and results. It is possible to consider contrasting values of parameters and vary the results which will be better for efficient design performances for engineers and disaster experts. To sum up, a real-time precise prediction may manifest great assistance in landslide occurrence forecasting.

5.6 Applicability of the proposed method

The presented case study and associated FEA present the capability of advanced numerical tools in modeling the slope failure and stability analysis. Some assumptions need to be made before the operating of a model like adjusting some of the hydrology factors which include the water table, overlying soil and bedrock characteristics, infiltration of rainwater, etc. Finally, the use of numerical models like FE can be time-consuming and complex, however, it is worthwhile. In this study, a rigorous numerical method using coupled hydro-mechanical analysis was used to determine the critical groundwater level, the effective stress, and strains, along with the total displacement. The results were matching with the real case, hence, the FEM model based on the hydro-mechanical constitutive model was appropriate for simulating the slope maneuvers.

This study has an important practical significance for engineers and researchers for providing the slope stability analysis and critical groundwater level for translational slide activation based on preliminary elevation, some geotechnical parameters, and rainfall data. They are useful for studying the ground hydrology and groundwater distribution control. Landslide analyses must be done with both prospective and retrospective methods for better accuracies. This study can inform engineers and disaster experts where and how to take mitigation measures to intercept a slope movement. For structural measures, piling or retaining walls can be constructed to reinforce the weak slopes. Sustainable land management and forest harvesting can help as long-term and economical initiatives for landslide prevention. It must be noted that for deep-seated landslides, engineering structures are not always successful and, in these cases, the sustainable development helps in mitigation.

5.7 Shortcomings and future scope

Numerical tools like FEM allow coupled stress-pore pressure-displacement analyses. However, it is difficult to capture the effects of tension cracks and soil inhomogeneity. It comprises fractures, cracks, macropores, and interaggregate pores. The presence of all these activities reduces the shear strength of soil slopes and increases the permeability of the soil. Numerical simulation of water flow in discrete fracture networks should be done in the future. Cracks and other soil features have an important influence on slope stability. Also, the weather conditions cannot be ignored. One should check the results and compare them with different rigorous techniques that satisfy all the conditions. A wide range of hydraulic properties is important for the prediction of the occurrence of deep-seated landslides. The heterogeneity of natural slopes is generally neglected. The outcomes change with the thicknesses of the sliding bodies, heterogeneity of the soil, inconsistencies of environmental conditions, variation of rainfall infiltration to recharge the GWL due to the different components of soil on different parts of the landslide bodies. The variation changes immensely with the change of each of these factors and must be included in future studies though it may extremely difficult to obtain. A huge expense of resources would be needed for obtaining a calibrated model if the heterogeneity is considered. A large number of uncertainties present in numerical analysis is one of the greatest problems affecting the accuracy and creating errors in simulations. These uncertainties will change and get reduced with the advancement of time and technology, and more robust engineering analysis will be possible. In the end, it must be said that engineering judgment is still essential, whichever method is used, whether it is a long-used popular method or a recent modified complex method.

Chapter 6 Conclusion

The contributions of this study can be summarized as follows:

1. The FE analysis is still one of the best methods for landslide analysis as it considers a vast number of parameters for prediction. The extra fine mesh analysis maybe time taking but the accuracy is satisfactory. The predicted values obtained from the study can be used for further advanced analyses.
2. From the results, the potential of the proposed method to analyze stability can be applied in practical design. The values predicted by the simulation can be used as critical value markers when developing early warning systems for landslide occurrence.
3. The various seepage and pore water flow lines obtained from the simulation gave the range of the GWLs where the landslide event is bound to happen. The probable CGWL present in this range plays a vital role in the occurrence of landslides.
4. This FE-SRM analysis exhibits the exact depth, the distance the sliding mass will cover, and the occurrence zone of the landslide beforehand. This can help as a pre-analysis prediction and the displacement marked areas can be reinforced by structural or vegetation systems.
5. The color variations shown in the von-mises stress and effective strain results show the variation of shear stress and strain along the model. The red areas indicated where the stress is maximum and going to rupture. It also revealed that the maximum stress was formed at the soil-bedrock interface.
6. The soil characteristics and mechanics also play an important role in triggering the landslide. The displacement analysis evaluated the range of distances for different layers of the landslide mass that travels downstream after the occurrence.

Several anticipation measures can be applied to the displacement zones found out from this proposed analysis i.e., modifying the slope geometry and reinforcing the soil body using piles, retaining walls and ground anchors, grouting rock joints and fissures, and diverting the debris flows.

7. After comparing the simulated model results with the Huisun area field elevation data, it was found that they conveyed a lot of similarities. Thus, it can be concluded that the simulation result is satisfactory and has good accuracy, thus can be used for real-time analysis.

8. During heavy rainfalls and typhoons there will be an abundance of rainfall and excessive infiltration of water which can trigger landslides and flooding in these areas. Building proper surface or underwater drainage systems along the slope surface is highly recommended. For example, creating an underwater tunnel along the flow lines to drain the excess infiltrated water or diverting the extra water to a large reservoir using spillways can also serve as water storage and can be used in the future when there is a shortage of freshwater supplies in Taiwan or other similar countries.

There have been many things that have been investigated and resolved while there are still some factors that are difficult to control or understand. Hence, research is important for uncovering the unknown. By evolving the known methods and factors the problem of landslides may get resolved completely in the future. Therefore, by researching we can better ourselves and reach near to the perfection of creating a perfect landslide warning system.

References

1. Baum, R. L., & Godt, J. W. (2010). Early warning of rainfall-induced shallow landslides and debris flows in the USA. *Landslides*, 7(3), 259-272.
2. Brown, D., Alvarez-Marron, J., Schimmel, M., Wu, Y. M., & Camanni, G. (2012). The structure and kinematics of the central Taiwan mountain belt derived from geological and seismicity data. *Tectonics*, 31(5).
3. Cai, F., & Ugai, K. (2004). Numerical analysis of rainfall effects on slope stability. *International Journal of Geomechanics*, 4(2), 69-78.
4. Cascini, L., Sorbino, G., Cuomo, S., & Ferlisi, S. (2014). Seasonal effects of rainfall on the shallow pyroclastic deposits of the Campania region (southern Italy). *Landslides*, 11(5), 779-792.
5. Chang, J. M., Chen, H., Jou, B. J. D., Tsou, N. C., & Lin, G. W. (2017). Characteristics of rainfall intensity, duration, and kinetic energy for landslide triggering in Taiwan. *Engineering Geology*, 231, 81-87.
6. Chen, C. W., Chen, H., Wei, L. W., Lin, G. W., Iida, T., & Yamada, R. (2017). Evaluating the susceptibility of landslide landforms in Japan using slope stability analysis: a case study of the 2016 Kumamoto earthquake. *Landslides*, 14(5), 1793-1801.
7. Collins, B. D., & Znidarcic, D. (2004). Stability analyses of rainfall induced landslides. *Journal of geotechnical and geoenvironmental engineering*, 130(4), 362-372.
8. COMSOL Multiphysics Reference Manual (2018).

9. Crosta, G. B., & Frattini, P. (2008). Rainfall-induced landslides and debris flows. *Hydrological Processes: An International Journal*, 22(4), 473-477.
10. Froude, M. J., & Petley, D. N. (2018). Global fatal landslide occurrence from 2004 to 2016. *Natural Hazards and Earth System Sciences*, 18(8), 2161-2181.
11. Gariano, S. L., & Guzzetti, F. (2016). Landslides in a changing climate. *Earth-Science Reviews*, 162, 227-252.
12. Gattinoni, P. (2009). Parametrical landslide modeling for the hydrogeological susceptibility assessment: from the Crati Valley to the Cavallerizzo landslide (Southern Italy). *Natural hazards*, 50(1), 161-178.
13. Geotechdata.info (2013-2021) <https://www.geotechdata.info/>
14. Ghiassian, H., & Ghareh, S. (2008). Stability of sandy slopes under seepage conditions. *Landslides*, 5(4), 397-406.
15. Griffiths, D. V., & Lane, P. A. (1999). Slope stability analysis by finite elements. *Geotechnique*, 49(3), 387-403.
16. Highland, L.M., & Bobrowsky, Peter. (2008). The landslide handbook – A guide to understanding landslides: Reston, Virginia, *U.S. Geological Survey Circular 1325*, 129 p.
17. Ho, C. S. (1986). A synthesis of the geologic evolution of Taiwan. *Tectonophysics*, 125(1-3), 1-16.
18. Hong, Y. M. (2017). Feasibility of using artificial neural networks to forecast groundwater levels in real time. *Landslides*, 14(5), 1815-1826.
19. Hong, Y. M., & Wan, S. (2011). Forecasting groundwater level fluctuations for rainfall-induced landslide. *Natural Hazards*, 57(2), 167-184.

20. Ishii, Y., Ota, K., Kuraoka, S., & Tsunaki, R. (2012). Evaluation of slope stability by finite element method using observed displacement of landslide. *Landslides*, 9(3), 335-348.
21. Jeong, S., Lee, K., Kim, J., & Kim, Y. (2017). Analysis of rainfall-induced landslide on unsaturated soil slopes. *Sustainability*, 9(7), 1280.
22. Labuz, J. F., & Zang, A. (2012). Mohr–Coulomb failure criterion. In *The ISRM Suggested Methods for Rock Characterization, Testing and Monitoring: 2007-2014* (pp. 227-231). Springer, Cham.
23. Lambe, T. W., & Whitman, R. V. (1991). *Soil mechanics* (Vol. 10). John Wiley & Sons.
24. Leshchinsky, B., Vahedifard, F., Koo, H. B., & Kim, S. H. (2015). Yumokjeong Landslide: an investigation of progressive failure of a hillslope using the finite element method. *Landslides*, 12(5), 997-1005.
25. Lu, N., & Godt, J. W. (2013). *Hillslope hydrology and stability*. Cambridge University Press.
26. Mansour, M. F., Morgenstern, N. R., & Martin, C. D. (2011). Expected damage from displacement of slow-moving slides. *Landslides*, 8(1), 117-131.
27. Mantovani, F., Pasuto, A., Silvano, S., & Zannoni, A. (2000). Collecting data to define future hazard scenarios of the Tessina landslide. *International Journal of Applied Earth Observation and Geoinformation*, 2(1), 33-40.
28. Matsui, T., & San, K. C. (1992). Finite element slope stability analysis by shear strength reduction technique. *Soils and foundations*, 32(1), 59-70.
29. Okeke, A. C. U., & Wang, F. (2016). Critical hydraulic gradients for seepage-induced failure of landslide dams. *Geoenvironmental Disasters*, 3(1), 1-22.

30. Pepper, D. W., & Heinrich, J. C. (2017). *The finite element method: basic concepts and applications with MATLAB, MAPLE, and COMSOL*. CRC press.
31. Pham, H. T., Oo, H. Z., & Jing, C. (2013). Stability of slope and seepage analysis in earth dam using numerical finite element model. *Study of Civil Engineering and Architecture (SCEA)*, 2(4), 104-108.
32. Pham, K., Lee, H., Kim, D., Lee, I. M., & Choi, H. (2018). Influence of hydraulic characteristics on stability of unsaturated slope under transient seepage conditions. *Landslides*, 15(9), 1787-1799.
33. Pradhan, S. P., Panda, S. D., Roul, A. R., & Thakur, M. (2019). Insights into the recent Kotropi landslide of August 2017, India: a geological investigation and slope stability analysis. *Landslides*, 16(8), 1529-1537.
34. Shao, W., Bogaard, T., & Bakker, M. (2014). How to Use COMSOL Multiphysics for coupled dual-permeability hydrological and slope stability modeling. *Procedia Earth and Planetary Science*, 9, 83-90.
35. Tsou, C. Y., Feng, Z. Y., & Chigira, M. (2011). Catastrophic landslide induced by typhoon Morakot, Shiaolin, Taiwan. *Geomorphology*, 127(3-4), 166-178.
36. Van Asch, T. W., Buma, J., & Van Beek, L. P. H. (1999). A view on some hydrological triggering systems in landslides. *Geomorphology*, 30(1-2), 25-32.
37. Wang, H., Zhang, B., Mei, G., & Xu, N. (2020). A statistics-based discrete element modeling method coupled with the strength reduction method for the stability analysis of jointed rock slopes. *Engineering Geology*, 264, 105247.

38. Wei, Z. L., Lü, Q., Sun, H. Y., & Shang, Y. Q. (2019). Estimating the rainfall threshold of a deep-seated landslide by integrating models for predicting the groundwater level and stability analysis of the slope. *Engineering Geology*, 253, 14-26.
39. Wei, Z. L., Wang, D. F., Sun, H. Y., & Yan, X. (2020). Comparison of a physical model and phenomenological model to forecast groundwater levels in a rainfall-induced deep-seated landslide. *Journal of Hydrology*, 586, 124894.
40. Wu, C. H., Chen, S. C., & Feng, Z. Y. (2014). Formation, failure, and consequences of the Xiaolin landslide dam, triggered by extreme rainfall from Typhoon Morakot, Taiwan. *Landslides*, 11(3), 357-367.
41. Yang, M. D., & Tsai, H. P. (2019). Post-earthquake spatio-temporal landslide analysis of Huisun Experimental Forest Station. *Terrestrial, Atmospheric & Oceanic Sciences*, 30(4).
42. Zhang, L. L., Zhang, J., Zhang, L. M., & Tang, W. H. (2011). Stability analysis of rainfall-induced slope failure: a review. *Proceedings of the Institution of Civil Engineers-Geotechnical Engineering*, 164(5), 299-316.
43. Zhou, C., Shao, W., & van Westen, C. J. (2014). Comparing two methods to estimate lateral force acting on stabilizing piles for a landslide in the Three Gorges Reservoir, China. *Engineering geology*, 173, 41-53.

Appendix

Appendix 1: Sieve analysis data

a) Point A:

Sieve no.	Sieve size(mm)	Mass of Soil retained(g)(W_i)	ΣW_i (g) (Cumulative weight)	f = $\frac{W_i}{W_o} \times 100(\%)$ Sieve sample percentage	(Cumulative residual rate) $R = \frac{\Sigma W_i}{W_o} \times 100$	Cumulative pass rate($D=100-R$)
#8	2.38	272.5	272.5	30.194	30.194	69.81
#16	1.19	214	486.5	23.712	53.906	46.094
#30	0.59	136	622.5	15.069	68.975	31.025
#50	0.297	90.5	713	10.028	79.003	20.997
#100	0.149	75	788	8.310	87.313	12.687
#200	0.074	47	835	5.208	92.521	7.479
Collector pan		67.5	902.5	7.479	100.000	0.000

b) Point B:

Sieve no.	Sieve size(m m)	Mass of Soil retained(g)(W_i)	ΣW_i (g) (Cumulative weight)	Sieve sample percentage	(Cumulative residual rate) $R = \Sigma W_i / W_o \times 100$	Cumulative pass rate(D=100-R)
#8	2.38	168	168	29.630	29.630	70.37
#16	1.19	112.5	280.5	19.841	49.471	50.529
#30	0.59	73	353.5	12.875	62.346	37.654
#50	0.297	82	435.5	14.462	76.808	23.192
#100	0.149	79.5	515	14.021	90.829	9.171
#200	0.074	32	547	5.644	96.473	3.527
Collector pan		20	567	3.527	100.000	0.000

c) Point C:

Sieve no.	Sieve size(m m)	Mass of Soil retained(g)(W_i)	ΣW_i (g) (Cumulative weight)	Sieve sample percentage	(Cumulative residual rate) $R = \Sigma W_i / W_o \times 100$	Cumulative pass rate(D=100-R)
#8	2.38	42.5	42.5	4.006	4.006	95.99
#16	1.19	134	176.5	12.630	16.635	83.365
#30	0.59	260	436.5	24.505	41.140	58.860
#50	0.297	284	720.5	26.767	67.908	32.092
#100	0.149	216.5	937	20.405	88.313	11.687
#200	0.074	74.5	1011.5	7.022	95.335	4.665
Collector pan		49.5	1061	4.665	100.000	0.000

d) Point D:

Sieve no.	Sieve size(m m)	Mass of Soil retained(g)(W_i)	ΣW_i (g) (Cumulative weight)	Sieve sample percentage	(Cumulative residual rate) $R = \Sigma W_i / W_o \times 100$	Cumulative pass rate($D=100-R$)
#8	2.38	171	171	10.888	10.888	89.11
#16	1.19	219.5	390.5	13.976	24.865	75.135
#30	0.59	288	678.5	18.338	43.203	56.797
#50	0.297	362	1040.5	23.050	66.253	33.747
#100	0.149	341.5	1382	21.745	87.997	12.003
#200	0.074	127.5	1509.5	8.118	96.116	3.884
Collector pan		61	1570.5	3.884	100.000	0.000